Space Science Reviews (2023) 219:63
https://doi.org/10.1007/s11214-023-01006-5

Understanding Active Region Origins and Emergence on the Sun and Other Cool Stars

Maria A. Weber[1] · Hannah Schunker[2] · Laurène Jouve[3] · Emre Işık[4,5]

Received: 27 May 2023 / Accepted: 15 September 2023 / Published online: 17 October 2023

Abstract
The emergence of active regions on the Sun is an integral feature of the solar dynamo mechanism. However, details about the generation of active-region-scale magnetism and the journey of this magnetic flux from the interior to the photosphere are still in question. Shifting paradigms are now developing for the source depth of the Sun's large-scale magnetism, the organization of this magnetism into fibril flux tubes, and the role of convection in shaping active-region observables. Here we review the landscape of flux emergence theories and simulations, highlight the role flux emergence plays in the global dynamo process, and make connections between flux emergence on the Sun and other cool stars. As longer-term and higher fidelity observations of both solar active regions and their associated flows are amassed, it is now possible to place new constraints on models of emerging flux. We discuss the outcomes of statistical studies which provide observational evidence that flux emergence may be a more passive process (at least in the upper convection zone); dominated to a greater extent by the influence of convection and to a lesser extent by buoyancy and the Coriolis force acting on rising magnetic flux tubes than previously thought. We also discuss how the relationship between stellar rotation, fractional convection zone depth, and magnetic activity on other stars can help us better understand the flux emergence processes. Looking forward, we identify open questions regarding magnetic flux emergence that we anticipate can be addressed in the next decade with further observations and simulations.

Keywords Sun · Solar · Sunspot · Magnetic field · Flux emergence

1 Introduction

The Sun is a magnetically active star showing activity on a wide range of spatial scales and field strengths. An active region is defined by the appearance of a dark feature at the surface of the Sun in continuum white light observations. These features are associated with concentrations of strong magnetic fields, and often develop into fully formed, stable sunspots. Typical active regions consist of opposite polarity pairs that are predominantly east-west aligned and have sizes ranging on the order of 10s to 100s of microhemispheres with lifetimes ranging from about two days up to many weeks.

Solar and Stellar Dynamos: A New Era
Edited by Manfred Schüssler, Robert H. Cameron, Paul Charbonneau, Mausumi Dikpati, Hideyuki Hotta and Leonid Kitchatinov

Extended author information available on the last page of the article

The Sun's coherent surface flux elements such as sunspots and active regions emerge from the solar interior. However, how they arrive at the surface and their specific depth of origin is not clear. Helioseismology has placed upper bounds on the amplitude and speed of the flows at and below the surface prior to emergence (e.g. Birch et al. 2013), however any unambiguous detection of flows above the background noise remains a challenge. Therefore, numerical simulations of flux emergence through the surface of the Sun are critical to reconciling the observations with the physics of the formation of active regions.

Originally, the paradigm of an idealized, magnetically isolated flux tube was invoked to model magnetism giving rise to active regions. Here, it is assumed that the dynamo has already managed to create magnetism at the base of the convection zone a priori. Studies employing this paradigm were first conducted using the thin flux tube approximation, which treats physical quantities as averages over the tube's cross-section (e.g. Spruit 1981; Fan et al. 1993; Caligari et al. 1995). This was followed by 2D (e.g. Moreno-Insertis and Emonet 1996; Fan et al. 1998) and 3D magnetohydrodynamic (MHD) (e.g. Abbett et al. 2001; Fan 2008) approaches to resolve the flux tube cross-section and twist of magnetic field lines. As a body of work, these simulations suggest that magnetic buoyancy, the Coriolis force, and the twist of magnetic field lines in a tube play roles in the flux emergence process and are responsible for many observed characteristics of active regions. Addition of a convection velocity field further demonstrated that turbulent interior flows modulate flux emergence, provided the magnetic field strength of the flux tube is not substantially super-equipartition (e.g. Fan et al. 2003; Jouve and Brun 2009; Weber et al. 2011). However, this paradigm of idealized flux tubes built by a deep-seated dynamo mechanism has been challenged by results from 3D global convective dynamo simulations. Some demonstrate that toroidal wreaths of magnetism can be formed within the bulk of a stellar convection zone (e.g. Brown et al. 2011; Nelson et al. 2011; Augustson et al. 2015; Matilsky and Toomre 2020). Either from these toroidal wreaths (Nelson et al. 2011, 2013) or more localized regions of strong toroidal field (Fan and Fang 2014) within the magneto-convection, buoyantly rising magnetic structures – possible starspot progenitors – are spawned. Results from both idealized flux tube simulations and the buoyant magnetic structures built self-consistently by dynamo action show similarities to active region observables, but there are also many discrepancies. Further modeling work with direct comparison to active region observations is critical to elucidate the true origin of active-region-scale magnetism.

The paradigm of the idealized, isolated flux tube mechanism for producing active regions is thus now changing towards a more complete picture. A large part of the recent paradigm shift was brought about from a statistical analysis of the flows associated with emerging active regions (e.g. Schunker et al. 2016; Birch et al. 2019), emphasising the importance of solar monitoring missions. Prior to instruments such as Helioseismic and Magnetic Imager (HMI) onboard NASA's Solar Dynamics Observatory (SDO) (Scherrer et al. 2012), with high duty-cycle observations of the magnetic field and Doppler velocity at a cadence sufficiently shorter than the time it takes an active region to emerge, it was not possible to gain any statistical understanding of the emergence process in such detail. Similarly, monitoring campaigns for stars e.g., Mt Wilson, *Kepler*, BCool, LAMOST, and TESS have increased both the sample size and the time range of data, such that magnetic variability has been measured over multiple cycle periods on other stars. Although the level of precision and sampling rate in such measurements are insufficient to amass emergence statistics for other stars like we have for the Sun, they help to shape our view over general trends of active-region formation in longitude and latitude, as well as the lifetimes of surface magnetic structures.

The longest record of the eleven-year activity cycle of the Sun is defined by the number of sunspots, or cool, dark regions, visible on the Sun. Active regions are defined from this

visible darkening when they are assigned an active region number by the National Oceanic and Atmospheric Administration. At the beginning of the solar cycle, sunspots appear at latitudes around 30°, and closer to the equator towards the end of the cycle, creating the observed butterfly diagram. Besides simply defining the solar cycle, active regions are found to have characteristics which correlate with the next solar cycle, suggesting that they are an integral part of the dynamo process. For example, the average tilt angle of sunspot groups over a solar cycle is anti-correlated with the amplitude of the next solar cycle (Dasi-Espuig et al. 2010; Jiao et al. 2021), and large active regions that emerge across the equator (e.g. Nagy et al. 2017) have a significant effect on the amplitude and duration of the subsequent solar cycle. Thus, to fully understand the dynamo process, it is critical to understand how active regions form.

Presumably the distribution of active regions on the surface of the Sun reflects the distribution of the global toroidal field in the interior (Işık et al. 2011), and can provide a strong constraint for their origin and the solar dynamo (e.g. Cameron et al. 2018). However, it cannot be excluded that the dynamo also produces strong field at latitudes which do not become unstable and rise to the surface. For other cool stars, the combined effects of rotation rate and fractional depth of the convection zone can lead to a possible mismatch between active regions on the surface and distributions of magnetic flux in the deeper interior due to latitudinal deflection as bundles of magnetism rise. As a result, any one-to-one association of observed surface field and the underlying dynamo in active cool stars is not necessarily straightforward (Işık et al. 2011). While it is not currently possible to directly observe the emergence of a starspot, it is possible to make proxy observations (e.g. from chromospheric indices, spectropolarimetry, Zeeman–Doppler imaging and asteroseismology; Berdyugina 2005; García et al. 2010; See et al. 2016) to infer the distribution, size, lifetime and magnetic field strength.

In this paper, we attempt to paint a comprehensive picture of the possible flux emergence process from generation of the active-region-scale magnetism in the deep interior to its appearance on the photosphere. We begin in Sect. 2, where we describe observations of the formation of active regions on the solar surface. These observations serve as inspiration and constraints for models of the generation and rise of emerging flux, which we review in Sect. 3. New observations are highlighted in Sect. 4, which support a more passive process for active region emergence than was previously understood based on flux emergence models. We then briefly review the role flux emergence plays in the solar dynamo process in Sect. 5, and discuss flux emergence leading to starspots on other cool stars in Sect. 6. In Sect. 7, we conclude with some recommendations as we move toward solving the active-region-scale flux emergence puzzle.

2 Formation of Active Regions at the Surface of the Sun

Active regions are defined by the appearance of dark spots on the visible disk of the Sun in white light, caused by strong, concentrated magnetic fields. The presence of this magnetism renders the spots cooler, and therefore darker, than the surrounding photosphere. Active region magnetic fields consist of roughly east-west aligned opposite polarity pairs, ranging from 10 up to 3000 micro-hemispheres in size, and 10^{20} to 10^{22} Mx of magnetic flux. Known as Hale's Law, bipolar active regions typically emerge with the same sign of the leading magnetic polarity in the same hemisphere, and the sign of the polarities are flipped in the opposite hemisphere (Hale et al. 1919). At the end of each 11-year sunspot cycle, the polarity orientation reverses for each hemisphere. In both hemispheres, active regions are roughly

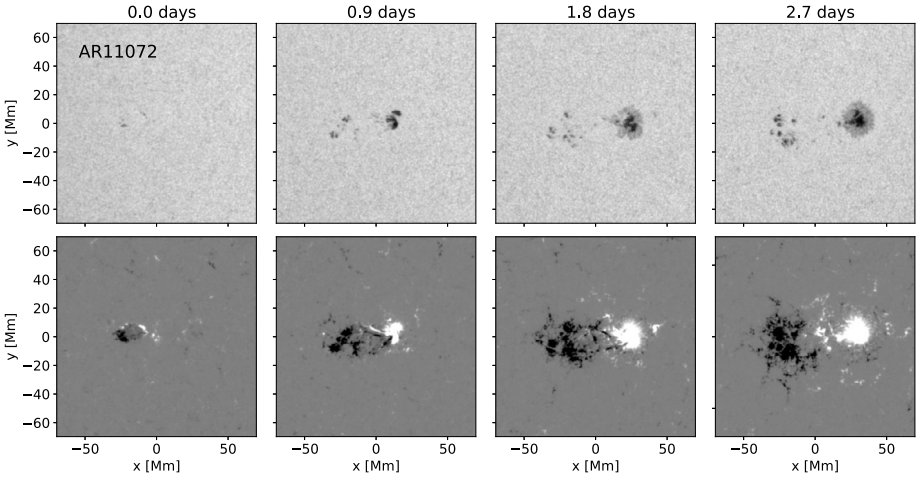

Fig. 1 Example of a typical active region, NOAA AR11072, emerging onto the surface of the Sun as observed by SDO/HMI. The top row shows Postel projected maps of the continuum intensity, and the bottom row shows maps of the line-of-sight magnetic field ±500 G. In this instance, 0 days corresponds to the emergence time 2010.05.20_17:12:00_TAI, and the maps are centred at Carrington longitude 316.43° and latitude −15.13°. The east-west direction is x and the north-south is y. Hale's Law, the formation of a sunspot in the leading polarity, and Joy's Law are evident

confined to toroidal bands of latitudes up to about 30°. They appear at higher latitudes at the beginning of each cycle and progressively closer to the equator over the duration of the roughly eleven year cycle.

The leading polarity of an active region (in the prograde direction) also tends to be closer to the equator than the following polarity (in the retrograde direction). This statistical feature is known as Joy's Law (Hale et al. 1919). Joy's Law is often quantified by the 'tilt angle' of the line drawn between the centers of leading and following polarity regions with respect to the east-west direction. Figure 1 shows the bipolar nature of a typical active region and illustrates Joy's Law, as the leading polarity of this southern-hemisphere active region is tilted closer to the equator.

An active region develops from a small magnetic bipole and grows in size as more and more magnetic flux emerges (e.g. Fig. 1). The flux-weighted centres of the polarities move further apart, predominantly in the east-west direction during the emergence process. The line-of-sight magnetic field observations show that magnetic field typically emerges as small scale features near the flux-weighted centre of the active region, which then stream towards the main polarities. Active regions have lifetimes on the order of days to weeks, where large, high-flux active regions live longer than small, low-flux regions (e.g. Schrijver and Zwaan 2000). Within the active regions, sunspots can form with peak magnetic field strengths from 2000 to 4000 G (e.g. Solanki 2003). Generally, the leading-polarity spot of the bipolar pair is larger and more coherent than the trailing-polarity region (see also Fig. 1). Active regions also have a preferred hemispheric sense of magnetic helicity, as obtained from vector magnetograms. The observations favor a left-handed (negative) twist of the field lines in the northern hemisphere, and a right-handed (positive) twist in the southern hemisphere (e.g. Pevtsov et al. 2001, 2003, 2014; Prabhu et al. 2020).

Having said how active regions *typically* form, there is a wide variation in characteristics. When two or more polarity pairs emerge in the vicinity of one another, the polarities can

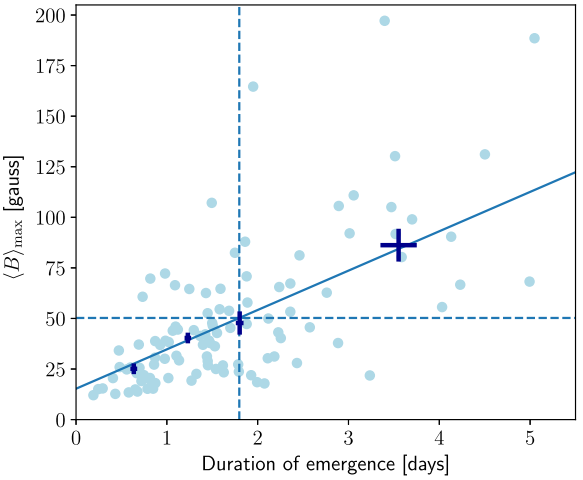

Fig. 2 Duration of the emergence process as a function of the maximum mean unsigned magnetic field $\langle B \rangle_{\max}$ for each emerging active region (light blue points) and the blue diagonal line is a linear fit with slope 19.5 ± 2.2 G/day. The blue horizontal dashed line is the mean of $\langle B \rangle_{\max}$, 48.6 ± 2.9 G, and the vertical dashed line is the mean duration of emergence time 1.7 ± 0.1 days. The mean and uncertainty values of $\langle B \rangle_{\max}$ bins with equal number of points are shown in dark blue. See Appendix 1 for details on how the emergence time was calculated

morph into the traditional bipolar structure during the emergence process, usually leading to a more complex, multi-spot active region (e.g. AR 11158 in Schunker et al. 2019, Fig. 1). It is also common to find active regions emerging into sites of existing magnetic field from previous active regions, so-called 'nests' of activity (Castenmiller et al. 1986), where the emerging magnetic field interacts via cancellation and superposition with the existing magnetic field.

Figure 2 shows that the duration of the emergence process until magnetic flux has stopped increasing is, on average, linearly proportional to the maximum mean unsigned magnetic field $\langle B \rangle_{\max}$ (see Appendix 1 for details on how the emergence time was calculated). Given that the maximum flux of an active region is known to directly correlate with the lifetime (e.g. Schrijver and Zwaan 2000), our results are consistent with Harvey (1993) (Chap. 3, Table III). Those results show that the "rise time" of active regions with a smaller maximum area is 1-2 days and increases to 3-4 days for active regions with larger maximum area (Harvey 1993). Here, we specifically avoid the term "rise time" since it implies a physical rising. What we are actually measuring is the time it takes magnetic flux to stop increasing in an active region at the surface. Figure 2 shows that the relationship is, though with considerable scatter, remarkably linear, with a slope of 19.5 ± 2.2 G per day.

As active regions are key observables for solar activity, any model of activity generation must reproduce the observed characteristics of the active regions.

3 Models of Emerging Flux

If the active-region-scale magnetism described in Sect. 2 is generated by the underlying dynamo, then it must somehow make its way from the subsurface large-scale magnetic field to the surface. The appearance of active regions evokes the idea of rising ropes of magnetism. We see arches of magnetic bundles extended above the Sun's surface. At the footpoint of these are sunspots. Within the Sun's interior is where we think these bundles of magnetic flux are born, which then rise and intersect with the photosphere to form sunspots. In this section, we briefly review models and their outcomes which describe the formation of active-region-scale magnetic structures and their rise to the photosphere (also see the reviews by Fan (2021) and by Cheung and Isobe (2014)).

3.1 Formation and Destabilization of Active-Region-Scale Magnetic Structures

The magnetism responsible for active regions is formed in the solar interior, however, the exact physical location of magnetic field generation is not known with certainty. There is a large body of work assuming that the magnetism giving rise to active regions is generated and stored at the base of the convection zone in the weakly subadiabatic overshoot region (e.g. Parker 1975; van Ballegooijen 1982; Moreno-Insertis et al. 1992; Rempel 2003). The tachocline is the name given to the region of radial and latitudinal shear at the interface between the solidly rotating radiative interior and the differentially rotating convection zone. Here it is thought that shear from differential rotation at the tachocline transforms poloidal field into toroidal field, which is amplified until it is strong enough to become buoyantly unstable. Then the magnetism subsequently rises through the convection zone to the photosphere. Beyond this shearing and storage mechanism, many studies of flux emergence, assuming the magnetism is formed as 'flux tubes' in the overshoot layer or at the very bottom of the convection zone, reproduce many properties of solar active regions (see 3.2).

Magnetic buoyancy instabilities have been considered as a means to initiate the rise of magnetic flux bundles from the overshoot region (e.g. Spruit and van Ballegooijen 1982; Spruit and van Vallegooijen 1982; Ferriz-Mas and Schüssler 1995; Caligari et al. 1995). Magnetic buoyancy is the result of a buoyant force due to the presence of a concentration of magnetism. Imagining this magnetism as a bundle or 'tube' of magnetic flux, there is a pressure balance between the gas pressure outside the tube (P_e) and the sum of the gas pressure (P_i) and magnetic pressure (P_b) inside. The gas density of the tube can be reduced if there is a condition of temperature equilibrium, allowing the tube to buoyantly rise (Parker 1955). Even if the tube is located in a subadiabatically stratified region and is in neutral density with its surroundings, a perturbation (e.g., in the transversal direction) could result in an undular instability that lifts part of the tube upward, creating an Ω-shaped loop, allowing mass to locally drain down the legs of the rising loop apex and initiating a buoyant rise. When considering thin flux tubes in mechanical equilibrium, their stability is primarily determined by their magnetic field strength and the subadiabaticity of the overshoot region (e.g. Caligari et al. 1995). It is found that the field strength of the flux tube must exceed the equipartition value of $\sim 10^4$ G by about an order of magnitude in order to develop unstable modes at sunspot latitudes in less than $\sim$1 year.

Instead of considering isolated magnetic flux tubes built in the tachocline region, many studies using multi-dimensional MHD simulations have focused on the formation of buoyant instabilities within layers of uniform, horizontal magnetic field. (e.g. Cattaneo and Hughes 1988; Matthews et al. 1995; Fan 2001; Vasil and Brummell 2008, 2009). Indeed, it has been shown that regions of velocity shear can generate tube-like magnetic structures or magnetic layers (e.g. Cline et al. 2003)). Vasil and Brummell (2008) find that a velocity shear representing a tachocline-like shear can generate a strong layer of horizontal magnetic field. From this self-consistently generated magnetic layer, buoyant structures resembling undulating 'tubes' arise due to magnetic buoyancy instabilities within the magnetic layer. However, the shear required to develop the magnetic buoyancy instabilities of the magnetic layer is much stronger and the magnetic Prandtl number is much larger than what is expected in the solar tachocline (Vasil and Brummell 2009). In order to generate a twist of the magnetic field within such rising magnetic 'flux tubes', as is found in active region observations, Favier et al. (2012) showed that it was sufficient to add a weak inclined uniform field on top of the unstable horizontal magnetic layer. Indeed, in this case, the unstable undulating tubes interact with the overarching inclined field as they buoyantly rise and the field lines start to wind around the tube axis, creating an effective twist in the magnetic structure.

There is now a shifting paradigm regarding the location of active-region-scale magnetic field generation. Recent global 3D magnetohydrodynamic (MHD) dynamo simulations have compelling outcomes which suggest that active-region-scale magnetism need not be formed at the base of the convection zone. In some, toroidal wreaths of magnetism exhibiting polarity cycles are built amid the magneto-convection without the need for a tachocline (e.g. Brown et al. 2011; Augustson et al. 2015). Taking similar simulations but reducing sub-grid-scale turbulent diffusion, Nelson et al. (2011, 2013, 2014) capture the generation of buoyant magnetic structures arising from magnetic wreaths – possible starspot progenitors. While typical azimuthal field strengths are a few kilogauss, buoyant loops are only spawned in regions with super-equipartition localized fields. The global dynamo simulations of Fan and Fang (2014) also exhibit super-equipartition flux bundles that rise toward the simulation upper domain. A common trait of these dynamo-generated buoyant loops is that they are continually amplified by shear and differential rotation as they rise. Unlike flux tube simulations (see 3.2), these are not isolated magnetic structures. Yet recently, Bice and Toomre (2022) found self-consistently generated flux ropes in a global 3D-MHD dynamo simulation representative of an early M-dwarf with a tachocline. The majority of the ropes remain embedded in the tachocline, while buoyant portions are lifted upward by longitudinally localized regions, or 'nests', of radial convection.

Taken together, these models and simulations of the formation and instability of buoyant magnetic structures, possible starspot progenitors, ask us to reconsider the paradigm of isolated magnetic flux tubes arising from the deep convection zone. However, as is the case with all simulations, it is important to note that all the simulations discussed here are far removed from the regime of real stars. For instance, thin flux tube models are very idealised and cannot treat the near-surface layers, while the 3D MHD models covering the entire convection zone do not yet reach magnetic Reynolds and Prandtl numbers of the solar convection zone. Yet, these simulations reproduce the observed properties of active regions remarkably well and give us a glimpse into the complex interplay of forces and mechanisms at work in stellar interiors that conspire to generate magnetic structures and facilitate their journey toward the surface.

3.2 The Flux Tube Paradigm

Isolated magnetic flux tubes in the convection zone have a long history of study because they are convenient both analytically and computationally, and had until recently been able to sufficiently explain the observed properties of active regions. In most studies, they are given an 'a priori' magnetic field strength and flux – it is taken for granted that the dynamo, via global or local processes, has somehow managed to create them - and usually assume they have been formed at the bottom of the convection zone. There are two primary types of flux tube simulations – the thin flux tube approximation (e.g. Spruit 1981; Fan et al. 1993; Caligari et al. 1995; Weber et al. 2011) and global 2D/3D MHD simulations (e.g. Emonet and Moreno-Insertis 1998; Fan et al. 2003; Fan 2008; Jouve and Brun 2009). The thin flux tube approximation takes the flux tube as so thin that there is an instantaneous balance between the pressure outside the flux tube and the gas pressure plus magnetic pressure inside the flux tube. All physical quantities are taken as averages over the tube cross-section, and the tube is essentially a 1D string of mass elements, free to be accelerated in three dimensions by bulk forces in ideal MHD, including buoyancy, magnetic tension, the Coriolis force (in the co-rotating frame), and aerodynamic drag. In order to resolve the flux tube cross section, 2D or 3D MHD simulations are used. These simultaneously solve the full set of MHD equations, and in some cases, convection. They often use the anelastic approximation, where

a background density variation is allowed in radius but in which sound waves are filtered out from the system. This approximation is perfectly valid within the solar interior. But to meet the grid resolution typical of these models, the flux tubes often have a flux too large for most active regions (see Fan 2021).

Flux tube simulations have sought to explain the appearance of solar active regions, such as their latitude of emergence, tilting action in accordance with Joy's Law, and the general trend of a more coherent, less fragmented morphology for the leading polarity of an active region as depicted in Fig. 1. For all of these examples, flux tube simulations have pointed toward the Coriolis force as the driver of the phenomenon. Consider three primary forces acting on a flux tube cross-section in the frame of reference co-rotating with the medium surrounding the tube: a magnetic tension force directed toward the Sun's rotation axis, a buoyancy force directed radially outward, and the Coriolis force acting on toroidal flows within the tube. As the tube traverses the convection zone, conservation of angular momentum drives a retrograde flow within the flux tube, resulting in a Coriolis force (as mentioned above) directed inward toward the rotation axis.[1] When the magnetic field strength of the flux tube is strong (i.e. super-equipartition), the buoyancy force dominates and the flux tubes rise radially from their original latitude at the base of the convection zone. As the initial field strength of the flux tube is decreased, the outward component of buoyancy diminishes compared to the inward component of the Coriolis force, and the resulting trajectory turns more poleward, such that flux avoids emerging at lower latitudes (e.g. Choudhuri and Gilman 1987; Caligari et al. 1995). A fourth force acting on the flux tube, the drag force, is stronger for flux tubes of lower magnetic flux. As a result, flux tubes with lower initial values of magnetic flux around 10^{20}–10^{21} Mx are able to rise more radially than those of 10^{22} Mx (e.g. Choudhuri and Gilman 1987; D'Silva and Choudhuri 1993; Fan et al. 1993).

If portions of the flux tube remain anchored deeper down in the convection zone, it is found within thin flux tube simulations that the material near the apex of a rising loop will both expand and diverge (although still with net retrograde motion), leading to a Coriolis force induced tilting of the loop toward the equator (D'Silva and Choudhuri 1993). Following the Joy's Law trend, these simulations also show an increasing tilt of the flux tube legs with increasing latitude of emergence (e.g. D'Silva and Choudhuri 1993; Caligari et al. 1995). This is expected if the Coriolis force is responsible for the tilting action, as the Coriolis force is proportional to the sine of the latitude. Additionally, the tilt angle is found to increase with increasing magnetic flux at fixed field strength (Fan et al. 1994). Within thin flux tube simulations, the retrograde plasma motion near the flux tube apex contributes to a stronger magnetic field strength in the leading leg (in the direction of solar rotation) compared to the following leg (e.g. Fan et al. 1993, 1994). It is noted that plasma is evacuated out of the leading flux tube leg into the following leg. Owing to the condition of pressure balance between the flux tube and its surroundings ($P_i + P_b = P_e$), this results in a stronger magnetic field strength for the leading side of the loop compared to the following (Fan et al. 1993; Caligari et al. 1995). Here it is important to highlight that idealized flux tube simulations of all varieties are very efficient at conserving angular momentum (e.g. Fan 2008; Jouve and Brun 2009; Weber et al. 2011), yet studies utilizing local helioseismology rules out the presence of retrograde flows on the order of 100 m/s, in favor of flows not exceeding $\sim$15 m/s (Birch et al. 2013). In comparison, the buoyantly rising magnetic structures within the 3D convective dynamo simulations of Nelson et al. (2014) are weakly retrograde and are

[1] This effect is thought to be responsible for the predominance of high-latitude spots on rapidly rotating active stars (see Sect. 6).

actually prograde within the simulations of Fan and Fang (2014). Within these 3D convective dynamo simulations, and perhaps within the Sun itself, flux emergence processes may deviate more from the 'idealized' flux tube paradigm than originally thought.

The twist of flux tube magnetic field lines in 2D and 3D MHD simulations has been found to be important for the coherent rise of the tube and consistent tilt angles. This body of work shows that if the magnetic field is not twisted enough along the flux tube axis, the flux tube tends to break apart and lose coherence as it rises (see review by Fan 2021). However, a radius of curvature in the rising Ω-shaped flux tube can partially mitigate this (e.g. Martínez-Sykora et al. 2015). Essentially, a minimum magnetic field twist rate (i.e. angular rotation of the magnetic field lines along the flux tube axis) is needed to counteract vorticity generation in the surrounding plasma caused by the buoyancy gradient across the flux tube's cross section. As discussed in Sect. 4.3, active region magnetic fields have been observed to have a preferred helical twist that is left-handed in the Northern hemisphere and right-handed in the Southern hemisphere (Pevtsov et al. 2003). But, Fan (2008) finds the tilt of the rising flux tube ends up in the wrong direction if the twist is of the observed preferred hemispheric sign and strong enough to maintain coherence of the flux tube. If the twist of the field lines is reversed in handedness, the tilt angle is of the correct sign. Reducing the magnetic field twist per unit length also solves the hemisphere tilt problem, but then the tube becomes less coherent and looses more flux as it rises.

The flux tube simulations mentioned previously in this section (3.2) do not consider the impact of convection on the evolution of rising magnetism. However, it is absolutely clear that convection modulates flux emergence when it is included, provided that the magnetic field is not substantially super-equipartition (e.g. Fan et al. 2003; Jouve and Brun 2009; Jouve et al. 2013; Weber et al. 2011, 2013b). Convective motions and magnetic buoyancy work in concert to promote flux emergence. Convection destabilizes the tube at the base of the convection zone, forcing parts to rise. As the tube bends, mass drains down the tube legs, making the apex less dense than portions deeper down, and that part of the tube also rises buoyantly. This, in combination with convective upflows, helps the flux tube to rise toward the surface, while convective downflows can pin parts of the flux tube in deeper layers. By embedding thin flux tubes in a rotating spherical shell of solar-like convection, Weber et al. (2013b) investigated how convection statistically impacts flux tube properties that can be compared to solar active regions. Taking all their results into consideration, they attempt to constrain the as-of-yet unknown dynamo-generated magnetic field strength of active-region scale flux tubes. They find that tubes with initial field strength $\geq$40 kG are good candidates for the progenitors of large (10^{21}–10^{22}) Mx solar active regions.

In particular, Weber et al. (2013b) find that convection tends to positively contribute to the Joy's Law trend, especially for mid-field-strength flux tubes of 40–50 kG. These flux tubes also take the longest time to rise due to the competing interplay of buoyancy and drag from surrounding turbulent flows. By 'increasing the Joy's Law trend', the authors refer to a systematic effect that the addition of solar-like giant cell convection tends to boost the tilt angle at the same emergence latitude compared to simulations not subject to a convective velocity field. This is attributed, in part, to the associated kinetic helicity within the upflows. Taking all of the simulations together for tubes initiated $\pm 40°$ degrees around the equator with a magnetic flux of 10^{20}–10^{22} Mx and initial field strengths of 15–100 kG, the distribution of tilt angles peaks around 10° degrees. This is in good agreement with the active region observations of Howard (1996) and Stenflo and Kosovichev (2012). Furthermore, similarly peaked tilt angle distributions are found for the buoyantly rising, dynamo-generated loops from the 3D convective dynamo simulations of Nelson et al. (2014) and Fan and Fang (2014). Perhaps this is indicative of similar processes at work in both these

convective dynamo simulations and the thin flux tube simulations of Weber et al. (2013b) – it is the turbulent, helical motion of convective upflows and the dynamics of the rising flux bundles themselves that contribute to the tilt angles extracted here.

3.3 Beyond Idealized Flux Tubes

In Sect. 3.2, we introduced the idealized flux tube paradigm to describe the transport of magnetism from the deep interior toward the surface. In Sect. 3.1, we noted that buoyantly rising magnetic structures have been found to arise from simulations of extended magnetic layers and form within wreaths of magnetism generated by dynamo action. In these latter two examples of MHD simulations, the buoyantly rising magnetism is *not* in the form of idealized, magnetically isolated magnetic flux tubes. While simulations of idealized flux tubes are able to reproduce some properties of solar active region observables (see Sect. 3.2), it may be unlikely that flux bundles rise within the convection zone entirely isolated from other nearby magnetic flux structures or a background field. Here we review studies of flux emergence that go beyond idealized flux tubes.

It is recognized that the presence of a background magnetic field and reconnection occurring between various magnetic flux structures have implications for the flux tube's evolution and the complexity of active regions. For example, Pinto and Brun (2013) introduce a twisted flux tube in a 3D spherical convection zone with an evolving background dynamo. In comparison to the purely hydrodynamic case of Jouve and Brun (2009), the presence of the background magnetic field introduces a 'drag' on the tube as it rises, which is dependent on the orientation of the flux tube's magnetic field with respect to the background field. In particular, flux tubes with one sign of twist seem to rise faster than the ones possessing the opposite sign. The favored handedness then depends on the preferred magnetic helicity sign of the dynamo field. By embedding a twisted toroidal flux tube in an effectively poloidal background magnetic field, Manek et al. (2018), Manek and Brummell (2021), Manek et al. (2022) show that a particular sign of twist increases the likelihood of a flux tube's rise and aligns with solar hemispheric helicity rules of active regions. Indeed, as mentioned in Sect. 2, observations show a tendency for active regions to possess a negative helicity in the Northern hemisphere and a positive one in the Southern hemisphere, although this is not a strict rule and only obeyed by only about 60% of active regions (Pevtsov et al. 2014).

Beyond the interactions between buoyant concentrations of magnetic field and the dynamo-generated smaller-scale fields, it has also been argued that the reconnections between multiple buoyantly rising structures could have strong consequences on emerging regions. In particular, these reconnections can be at the origin of complex active regions, with strongly sheared polarity inversion lines and patches of positive and negative magnetic helicity, indicating a high potential for flaring activity. Simulations of such processes were conducted initially by Linton et al. (2001) in a Cartesian geometry and then by Jouve et al. (2018) in a spherical shell including convection. In the latter, it was found that flux tubes with the same sign of axial field and same twist could merge to produce a single active region with a complicated structure and non-neutralized radial currents which could make these regions more likely to produce flares. Fully compressible calculations by Toriumi et al. (2014) were also performed to explore the possibility that the intense flare-productive active region NOAA 11158 could be the product of interacting buoyant magnetic structures.

The global models which simulate the interactions between convective motions, large-scale flows and more-or-less idealized, isolated magnetic flux tubes do not treat the uppermost layers of the convection zone and thus do not model the photospheric emergence. Firstly, the thin flux-tube approximation loses its validity above $\sim 0.98\ R_\odot$, owing to the

expansion of the tube apex to maintain pressure balance, to the extent that the tube radius becomes comparable with the local pressure scale height. Secondly, the anelastic approximation also breaks down close to the photosphere where Mach number becomes of order unity. At this point, as a caution to the reader, we have to remember that the outcomes from these computational simulations serve only as touchstones for comparison to active regions. Direct comparisons between the properties of observed active regions and the results of thin flux tube simulations, as well as the magnetic bipolar structures produced at the top of the computational domain of 3D anelastic simulations, may be misleading.

Compressible simulations including radiative transfer more closely approach the physics occurring at the top of the convection zone. These simulations aim at understanding how buoyant magnetic structures would make their way through the huge gradients of density and temperature in this region. This work first started with Cheung et al. (2010) who used the MURaM code (Vögler et al. 2005) to simulate the photospheric emergence of a highly twisted semi-torus placed at the base of the computational domain (around 7 Mm below), which was then gently brought towards the surface by an imposed radial velocity field of 1 km/s. This work was then extended to investigate the effects of other geometric structures of magnetic fields introduced at the bottom of the domain. In particular, Chen et al. (2017) used the flux concentrations produced by the convective dynamo simulations of Fan and Fang (2014) as an input, with a significant rescaling of the magnetic flux contained in these concentrations to have values at the photosphere compatible with typical active regions. Subsequently, an active-region-like structure was formed.

Another example employing the MURaM code are the near-surface simulations of Birch et al. (2016), where a half torus of magnetic field, without twist, is introduced through the bottom boundary with varying speeds, up to the $\sim$500 m/s predicted rise speed of a thin flux tube (Fan 2008). They found that the strong diverging flows at the surface for structures rising quickly are incompatible with observations, which do not show a significant diverging flow when they emerge.

Using the STAGGER code to model compressible, radiative MHD of the near-surface Stein and Nordlund (2012) introduced an even less structured magnetic concentration by only imposing a relatively weak untwisted uniform horizontal field of 1 kG at the bottom boundary (at 20 Mm blow the surface). This field then rises towards the photosphere at the convective upflow speed and self-organizes into a bipolar region with one coherent polarity and one more dispersed polarity. Several observational aspects like the rise speed, the absence of a strong retrograde flow, and the asymmetry between the polarities are reproduced in these simulations.

Other types of simulations of highly stratified turbulence also spontaneously produced magnetic flux concentrations resembling active regions, albeit not at the spatial or flux scales of real active regions, without the need to advect a well-defined magnetic structure at the bottom of the domain. It is the case for example of simulations by Brandenburg et al. (2013) and then Käpylä et al. (2016) where the Negative Magnetic Pressure Instability (NEMPI) mechanism is invoked to explain the spontaneous clumping of magnetic fields into a coherent structure. The most important ingredients in such simulations seem to be the strong density stratification and the large degree of turbulence. The formation of active regions following such a mechanism would then imply that they are produced in the subsurface layers of the Sun where both strong stratification and turbulence exist. If it turns out that such mechanisms are indeed at work in the Sun, this would completely revise our understanding of the flux emergence process and its origin. However, it is yet unclear if the NEMPI would still occur in more realistic conditions (Käpylä et al. 2016) or how observed active region properties such as Joy's Law might be reproduced via this mechanism.

The flux emergence process spans many orders of magnitude of density scale heights. Owing in part to this, it is difficult to get one singular simulation that tracks flux emergence from its generation by the dynamo to its interaction with the photosphere. As described above, some work has been done to 'couple' flux emergence simulations of the deeper interior with those of a photosphere-like region. Hotta and Iijima (2020) performed the first radiative MHD simulation of a rising flux tube in a deep convection zone, although without rotation, up to the photosphere. A 10 kG flux tube is introduced at 35 Mm below the top domain. Convection then modulates the flux tube, resulting in magnetic 'roots' anchored in two downflows as deep as 80 Mm with a bipolar sunspot-like region forming at the apex of the now Ω-shaped flux bundle. More realistic simulations like these, incorporating rotational effects, will make it increasingly straightforward to directly compare to, and interpret, solar observations.

4 Observational Constraints Supporting a Passive Active Region Emergence

The formation of each active region is unique. Simulations of active region emergence, especially those in 3D with appropriate active-region-scale magnetic flux, are currently too computationally expensive to build a statistically significant sample of flux emergence scenarios (although Weber et al. 2011, 2013b, have circumvented this somewhat by performing simulations of thin flux tubes embedded within a time-varying 3D convective velocity field; see Sect. 3.2). This limiting factor makes it especially important to have a comprehensive sample of observed emerging active regions for comparison. Understanding the common properties of the emergence process is the only avenue to constrain the common physics behind flux emergence. There have been a number of statistical observational studies (e.g. Komm et al. 2008; Kosovichev and Stenflo 2008; Leka et al. 2013; Birch et al. 2013; Barnes et al. 2014; McClintock and Norton 2016) on the formation of active regions, but in this paper we will focus on the observed characteristics that can place direct constraints on the models. We refer to an 'active' emergence as being guided by the magnetic field, and 'passive' as being guided by the convection.

4.1 Geometry of the Flux Tube

There is an apparent asymmetry in the east-west proper motions of the two main active region polarities as they emerge, with the leading polarity moving prograde faster than the following polarity moves retrograde (e.g. Gilman and Howard 1985; Chou and Wang 1987). Simulations have explained this as consistent with a geometrical asymmetry in the legs of an emerging flux tube, where the leg in the prograde direction is more tangentially oriented than the following leg which is more radial (see for example Fig. 5 of Jouve et al. 2013). As this flux tube rises through the surface, the leading polarity moves more rapidly in the prograde direction than the following polarity in the retrograde direction. Modeled within the thin flux tube approach in particular, this asymmetry is due to the Coriolis force driving a counter-rotating motion of the tube plasma so that the summit of the loop moves retrograde relative to the legs (e.g. Moreno-Insertis et al. 1994; Caligari et al. 1995).

However, Schunker et al. (2016) showed that while there is an apparent asymmetry of the leading and following polarity motion of the active region with respect to the Carrington rotation rate, this east-west motion is actually *symmetric* with respect to the local rotation speed following the differential rotation profile as described by Snodgrass and Ulrich (1990).

Here, in Fig. 3 we show the separation velocities for 117 active regions (more than the sample in Schunker et al. (2016)) further supporting the initial results. The average motion of the leading and following polarities in the first day after emergence is asymmetric with respect to the Carrington rotation rate (Fig. 3, left), consistent with e.g. Chou and Wang (1987), where the mean east-west velocity of the leading polarity in the first day after emergence is 127 ± 14 ms^{-1} and the trailing polarity is -61 ± 10 ms^{-1}. However, we emphasise that *the east-west motion of the polarities about the local plasma rotation speed is symmetric* (Fig. 3, right).

While not related to the east-west motion of the individual polarities, Weber et al. (2013b) showed that by embedding thin flux tubes within solar-like convection, the average rotation rate of the center between the flux tube legs can approach the surface plasma rotation rate. However, this only occurs for strong flux tubes with initial field strengths of $\geq$60 kG, which exceeds the magnetic field strength in equipartition with convection ($\sim$10 kG) near the base of the convection zone (see e.g. Weber et al. 2011). Furthermore, due to strong conservation of angular momentum within the rising loop, the plasma flow at the apex of the loop is substantially retrograde (see also Sect. 3.2), in contrast to observations (Birch et al. 2013).

Based upon these outcomes from observations and simulations, we suggest that any constraints placed on models of emerging flux tubes with geometrically asymmetric legs should be carefully reconsidered. Care should also be taken when choosing the particular reference frame to study the motion of the polarities.

4.2 Rise Speed of the Flux Tube

In the absence of convection, idealized thin flux tube simulations show an upward rise speed of about 500 m/s at about 20–30 Mm below the surface (e.g. Caligari et al. 1995). To understand how this would manifest at the surface of the Sun, Birch et al. (2016) inserted a half torus of magnetic flux with a rise speed of 500 m/s through the bottom boundary of a three-dimensional, fully convective, near-surface simulation. This simulation produced a strong horizontal outflow at the surface (about 400 m/s) as it emerged. Observations of the surface flows during an emergence on the Sun do not show such a strong outflow signature, but rather flow velocities that are consistent with a rise-speed less than $\sim$100 m/s, typical of convective upflows in the near-surface layers. In agreement with the observations, a flux tube that emerges naturally from a depth of 50 Mm within the radiative MHD simulations of (Hotta and Iijima 2020) does not produce any significant outflow at the surface. However, the rise speed of the flux tube is 250 m/s. This calls into question the traditional, idealized flux tube picture and suggests that the convection has an influence on the near-surface emergence process, but does not exclude thin flux tubes which may rise from the base of the convection zone with a slower speed.

Hotta and Iijima (2020) suggest that the reason their flux tube forms such a convincing active region structure is because it is initially placed across two coherent downflow regions. The downflows effectively pin the ends of the flux tube down, so that the centre emerges as a loop, implying that the influence of convection extends down to where flux tubes lie, and even instigate the emergence process, supporting some of the global models. Such correlations between rising (sinking) parts of flux tubes and upflows (downflows) were already observed in models of emergence in the bulk of the convection zone (e.g. Fan et al. 2003; Weber et al. 2011, 2013b) and in rising flux bundles generated within 3D convective dynamo simulations (Nelson et al. 2011, 2013; Fan and Fang 2014). However, the work of Hotta and Iijima (2020) shows that this interplay could also happen near the photosphere and highlights the potential importance of convective motions to bring the observed magnetic structures to the surface.

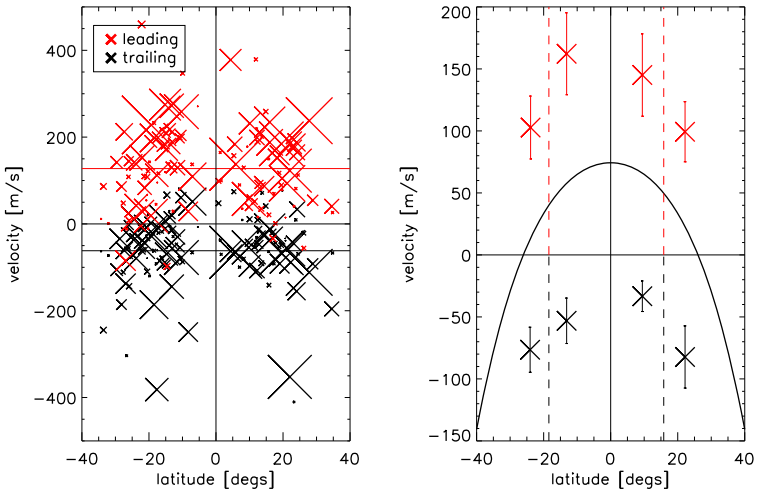

Fig. 3 Left: The mean east-west velocity relative to the Carrington rotation rate of the leading (red crosses) and trailing (black crosses) polarities over the first day after emergence for 117 active regions selected from the Solar Dynamics Observatory Helioseismic Emerging Active Regions Survey (SDO/HEARS; see Table A.1 in each of Schunker et al. (2016, 2019) for a full list of active regions in SDO/HEARS and Appendix 1 for a list of active regions that were excluded). The size of the symbols represents the size of the active region (AR 11158 is the largest). The scatter is large; this emphasises the unique nature of each active region emergence. The mean velocity of the leading polarity in the first day after emergence is 127 ± 14 ms^{-1} and the trailing polarity is -61 ± 10 ms^{-1} . Right: The average velocities in bins of polewards and equatorwards latitudes divided by the median latitude (dashed vertical lines) of the EARs. The black curve shows the differential velocity of the surface plasma relative to the Carrington rotation rate. The uncertainties are given by the rms of the velocities in each bin, divided by the square root of the number of EARs in the bin. This figure is an updated version of Fig. 11 in Schunker et al. (2016) where the average speed of the leading polarities was 121 ± 22 ms^{-1} and for the trailing polarities was -70 ± 13 ms^{-1}. Full details of the method to measure the east-west polarity speeds are described in Sect. 7 of Schunker et al. (2016)

4.3 Onset of Joy's Law

Joy's Law is the observed tendency of the leading polarity in predominantly east-west aligned active regions to be slightly closer to the equator than the following polarity. The angle these polarities make relative to the east-west direction is called the tilt angle, and it increases with the latitude of the active region, strongly suggesting that Joy's Law has its origins in the Coriolis force. In some mean-field dynamo models, Joy's Law is an important characteristic where the tilt angle acts as a non-linear feedback mechanism (e.g. Cameron et al. 2010).

Within the idealized flux tube paradigm, plasma near the rising flux tube apex will expand and diverge. This results in a Coriolis force-induced tilt of the tube axis in the sense of Joy's Law that increases with latitude (see Sect. 3.2). In this picture, the tilt angle should be present at the time of emergence. The tilt angle also depends on the flux and field strength of the magnetism (e.g. Fan et al. 1994). A larger magnetic flux, Φ, increases the buoyancy of the tube, and therefore the rise speed and effect from the Coriolis force, such that the tilt angle, α, increases for fixed magnetic field strength B ($\uparrow \Phi_{B=\text{fixed}} \Rightarrow \uparrow \alpha$, or, the thicker the tube, the larger the tilt angle). But larger magnetic field strength (for the same flux) increases the magnetic tension of the flux tube, which decreases the tilt angle due to the domination of tension over the Coriolis force ($\uparrow B_{\Phi=\text{fixed}} \Rightarrow \downarrow \alpha$, for fixed cross-sectional radius, see also Işık 2015).

Weber et al. (2013b) show that incorporating the effects of time-varying giant cell convection systematically increases the tilt angles of rising flux tubes compared to the case without convection, but does not necessarily reproduce the tilt angle trends as found in Fan et al. (1994) (also see Sect. 3.2). However, they do note that there is a larger spread in tilt angles at lower magnetic flux, as reported in some observations (e.g. Wang and Sheeley 1989; Stenflo and Kosovichev 2012). Taken together, these simulation results show that the interplay of time-varying convection, the Coriolis force, magnetic tension, and buoyancy are all factors that could influence the tilt angle of active regions on the Sun.

Schunker et al. (2020) measured the tilt angle of over 100 active region magnetic polarities throughout the emergence process, and found that on average, the polarities tend to emerge east-west aligned (i.e., with zero tilt), albeit with a large scatter, and the tilt angle develops during the emergence process. Moreover, Schunker et al. (2020) found that the latitudinal dependence of the tilt angle arises only from the north-south motion of the polarities, and the east-west motion is only dependent on the amount of flux that has emerged. They also found that there was not a statistically significant dependence of the tilt angle on the eventual maximum magnetic flux of the active regions. Schunker et al. (2020) conclude that the observed Joy's Law trend is inconsistent with a rising flux tube that has an established, latitudinally dependent tilt angle as it rises to intersect with the photosphere. We note that idealized thin flux tube models do not extend all the way to the surface (typically $\approx$0.98 $R_{\odot}$) where convection becomes important, however in simulations of coherent magnetic structures rising through the near-surface convection, the surface signature still reflects the orientation of the subsurface footpoints (e.g. Chen et al. 2017).

Another possibility to explain Joy's Law is the conservation of magnetic helicity in a flux tube as it rises through the surface (e.g. Berger and Field 1984; Longcope and Klapper 1997). The magnetic helicity is composed of the writhe, which measures the deformation of the flux tube axis, and the twist of the magnetic field lines about the axis. Ideally, the magnetic helicity is a conserved quantity, and changing one component necessarily requires a change in the other. In some simulations, the twist of the magnetic field about the axis of the flux tube is vital to it remaining coherent as it rises (e.g. Fan et al. 1998; Fan 2008). Within the thin flux tube context, it is shown that the writhe developed by the evolving flux tube can generate local magnetic field twist (Longcope and Klapper 1997; Fan and Gong 2000), a phenomenon which Longcope et al. (1998) term the Σ effect (see also Cheung et al. 2017). However, this effect alone is not enough to account for the observed twist of active regions (see Fan 2021). Indeed, this relationship between the twist of the magnetic field and the writhe of the flux tube (related to the tilt of the active region) has been posited as a means to explore the link between 'kink unstable' flux tubes and complex sunspot groups that have polarity orientations opposite to Hale's Law (e.g. Fuentes et al. 2003; Fan 2021). While there have been multiple studies of the helicity and twist of the surface magnetic field in active regions (e.g. Pevtsov et al. 2014, and references therein), the relationship between the twist and writhe is still ambiguous. This is probably because observations do not have access to the full three-dimensional structure of the magnetic field above the surface; only proxies for the twist (e.g. Baumgartner et al. 2022) and estimates of the helicity can be measured.

An interesting proxy for the global twist and writhe in active regions is the presence of so-called magnetic tongues (see Fig. 4, left). These structures are due to the fact that the polarities of active regions appear elongated in line-of-sight magnetograms during their emergence (López Fuentes et al. 2000). The elongation is thought to be produced by the line-of-sight projection of the azimuthal magnetic field at the peak of a twisted emerging flux-tube as it emerges through the surface. Thus, it is a proxy for the net twist of the active

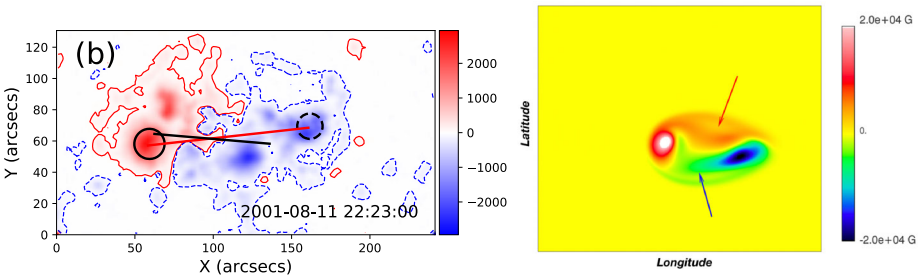

Fig. 4 Left: Example of magnetic tongues observed by SOHO/MDI on the active region 9574. The blue and red shaded areas correspond to negative and positive values of the line-of-sight magnetic field (in units of gauss) and the black circles indicate the positions of the core flux of each polarity. Right: Example of magnetic tongues simulated in a global 3D MHD model of a twisted Ω-shaped loop magnetic structure emerging close the top of the spherical shell (here $r = 0.9\ R_{\odot}$). Red and blue colours correspond to positive and negative radial magnetic fields and the arrows indicate the tongues of each polarity. ©AAS. Reproduced by permission from Poisson et al. (2020) (left panel) and Jouve et al. (2013) (right panel)

region flux tube, and coupled to the orientation of the polarities (as a proxy for writhe), gives a constraint on the magnetic helicity brought to the photosphere by the emergence process (Luoni et al. 2011). As the emergence proceeds, the tongues will vanish as the peak of the flux tube passes the surface and the legs of the flux tube remain. A less-biased measurement of the tilt angle will then be accessible. Magnetic tongues have also been reproduced in 3D MHD simulations where a twisted flux tube emerges through the deeper solar interior (e.g. Jouve et al. 2013, and Fig. 4, right) and closer to the photosphere (e.g. Archontis and Hood 2010; Cheung et al. 2010). Again, a clear relationship can be established between the direction of elongated tongues and the sign of the global active region twist, similarly to what is found in observations (Poisson et al. 2022).

The cycle-averaged tilt angles of sunspot groups show anti-correlation with the amplitude of the cycle (Dasi-Espuig et al. 2010; Jiao et al. 2021), also known as tilt quenching (see also Jha et al. 2020). A surface mechanism that explains this phenomenon is driven by inflows in the north-south direction towards active belts around the equator, effectively pushing the latitudinal separation of active regions polarities closer together (Jiang et al. 2010; Cameron and Schüssler 2012). In the idealized thin flux tube picture, the same effect is consistent with enhanced cooling near the base of the convection zone, where the strong toroidal flux is thought to be stored (Rempel 2003; Işık 2015): this cooling stabilizes the overshoot layer, shifting the onset of the magnetic buoyancy instability to higher field strengths, which increases the magnetic tension in the rising flux tube, which in turn quenches the tilt angle at the emergence (Işık 2015). The magnitude of local cooling is proportional to the amount of magnetic flux in the overshoot region. Global helioseismic estimation of the sound-speed change from minimum to maximum of an activity cycle (Baldner and Basu 2008) implies a degree of cooling at the base of the convection zone that is consistent with the rates required to yield the observed cycle-to-cycle changes of the mean tilt angle.

An important task for future numerical simulations then is to decide to which extent Joy's law arises from (1) the latitude-dependent Coriolis force induced by diverging flows near the tube apex below the surface (ie, angular momentum conservation of horizontally diverging flows on a rotating fluid), (2) the interplay among twist, writhe and magnetic tension, and (3) the convective flows, which impose the tilt on flux bundles.

5 Flux Emergence and the Solar Dynamo

5.1 Crucial Role of Active Regions in Global Field Reversals

The magnetic flux that emerges through the photosphere in the form of bipolar magnetic regions is likely to play a key role in recycling the global magnetic field of the Sun. The idea that flux emergence as tilted bipolar active regions could play an active part in the dynamo process dates back to the 1960s with the seminal works of Babcock (1961) and Leighton (1969). Indeed, in the so-called Babcock–Leighton (BL) model, the large-scale poloidal field owes its origin to the decay of sunspots at the photosphere. The leading polarity, closer to the equator, partially cancels with the opposite polarity in the other hemisphere, leaving a net flux to diffuse towards the pole to reverse the polar field of opposite sign. An important ingredient has then been added to this model – the large-scale meridional flow observed in the uppermost part of the convection zone (Gizon et al. 2020). These models including this flow are known as flux-transport dynamo models and are reviewed in another article of this collection (Hazra et al. 2023).

Recently, Cameron and Schüssler (2015) applied Stokes' theorem on the meridional plane of the Sun encompassing the convection zone to show that the net toroidal flux generated by differential rotation must arise solely from the magnetic flux emerging at the surface. That surface flux mainly stems from the dipole moment contribution to the poloidal field of the Sun, which the tilted active regions eventually produce in the course of an activity cycle (Cameron et al. 2018). This theoretical finding highlighted the importance of flux emergence in solar and stellar dynamo processes. Indeed, similar analysis has been conducted by Jeffers et al. (2022) on two active K-dwarf stars followed by spectropolarimetry (ϵ-Eridani and 51 Cygni A) where, similarly to the Sun, a balance is found between the generation of toroidal flux associated with the poloidal field threading through the stellar surfaces and the loss of magnetic flux associated with flux emergence.

The latitudinal distribution and the tilt angle of emerging active regions thus seems to be of utmost importance in determining the global axial dipole of the Sun. As discussed in Sect. 4.3, cycle-averaged tilt angle of sunspot groups are reported to show anti-correlation with the cycle strength (Dasi-Espuig et al. 2010; Jiao et al. 2021). This tendency has been interpreted as a manifestation of nonlinear saturation of the solar cycle. Accordingly, the effect works so as to limit further growth of the toroidal flux of the subsequent cycle. It does so by quenching the surface source for the global axial dipole moment through a lower average tilt angle of active regions. To account for the systematic effect, two physical mechanisms have been suggested: convergent flows towards emerged active regions, with the velocity depending on cycle strength (Jiang et al. 2010; Cameron et al. 2010), or a deep-seated stabilisation of flux tubes by cooling, the extent of which depends on the toroidal magnetic flux (Işık 2015, see Sect. 4.3).

Although most global MHD dynamo simulations producing large-scale magnetic cycles (e.g. Ghizaru et al. 2010; Nelson et al. 2013; Käpylä et al. 2012; Augustson et al. 2015; Hotta et al. 2016; Strugarek et al. 2017) do not extend to the photosphere, the top magnetic field boundary generally assumes a radial field or connects to a potential magnetic field. Thus, magnetic flux that reaches the top boundary is allowed to thread through the surface, producing the necessary radial magnetic field distribution that is crucial for the generation of the net toroidal flux (as described in Cameron and Schüssler 2015). However, what is still missing in those simulations is the formation of explicit starspots at the photosphere. Global dynamo simulations with more realistic near-surface layers and treatment of active-region-scale flux emergence would be ideal to better understand the physics of the emergence process.

5.2 Incorporating Flux Emergence in Babcock–Leighton Dynamo Models

Following the idea that flux emergence could play a key role in the dynamo process and that full 3D MHD global models do not yet capture all the characteristics of flux emergence, some works have been devoted to take prescriptions coming from 3D models of flux emergence and incorporate them into 2D mean-field Babcock–Leighton model. This was done, for example, in Jouve et al. (2010). Here, the idea was to take into account the fact that flux tubes do not rise instantaneously to the surface (contrary to what is assumed in the standard BL model) and that the rise speed is a non-linear function of the magnetic field strength. They found that this small (but non-linear) delay in the rise time of flux tubes could produce long-term modulation of the cycle amplitude and phase.

Recently, the idea of combining the outcomes of 3D flux emergence simulations and 2D BL models has been used to produce new 3D flux-transport BL dynamo models, where active regions would be formed according to the toroidal field self-consistently created by the shearing of the poloidal field at the base of the convection zone (Yeates and Muñoz-Jaramillo 2013; Miesch and Dikpati 2014; Kumar et al. 2019; Pipin 2022; Bekki and Cameron 2023). These new models are particularly promising to study the role of active regions in the reversal of the polar magnetic field in the Sun and possibly other cool stars. Indeed, one of their advantages is that they are less prone to the caveat of 2D models of producing too much polar flux compared to observations. Moreover, in the last two references cited above, the non-linear feedback of the Lorentz force on the large-scale flows is taken into account and the impact of flux emergence on differential rotation and meridional flows can then be assessed. As further proof on the importance of active region tilt angles on the reversal of the Sun's poloidal field, Karak and Miesch (2017) find that introducing a tilt angle scatter around the Joy's Law trend in a 3D BL dynamo induces variability in the magnetic cycle, promoting grand maxima and minima. Many improvements still need to be implemented in these models, by incorporating statistics of flux emergence and characteristics of mean flows even closer to observations for example and possibly by implementing data assimilation techniques to construct predictive models for future solar activity (see recent review by Nandy 2021, on this subject). Another improvement could also be to adapt these models to other stars with various emergence characteristics. Nonetheless, simplified 3D BL models are already very valuable tools to be used before full 3D MHD models of spot-producing dynamos can be constructed.

6 Flux Emergence on Other Cool Stars

6.1 Some Clues from Observations

Most stars with outer convection zones are capable of generating strong magnetism leading to starspots (e.g. Berdyugina 2005; Strassmeier 2009). The emergence of magnetic regions on other stars is not directly observable, however the strength and distribution of magnetic flux on the surface of stars can be inferred from observations such as light-curve variability, (Zeeman-)Doppler imaging, and interferometry (see also van Saders et al. in this volume). This is only possible for stars significantly more active than the Sun, and it would not be possible to measure these properties treating the Sun as a star. The general trend for Sun-like stars is that for a given effective temperature, the unsigned surface magnetic flux increases with rotation rate until reaching a saturation point for faster rotators (e.g. Reiners et al. 2022). There is also a preference for faster rotators to exhibit higher-latitude spots (e.g.

Berdyugina 2005), but some rapidly rotating stars and fully convective M dwarfs can exhibit spots simultaneously at high and low latitudes (e.g. Barnes et al. 1998; Jeffers et al. 2002; Barnes et al. 2015; Davenport et al. 2015).

It is then natural to wonder whether the observed trends of magnetic flux result from a link between the generation of the large-scale toroidal magnetic field and the bulk rotation rate. Stellar rotation and effective temperature also affects the amplitude, vorticity, and turn-over time of the convection; in turn impacting the star's differential rotation (i.e. shear) profile (see e.g. Brun and Browning 2017, and references therein). Some mean-field dynamos of the Sun incorporating a solar differential rotation profile find toroidal magnetic field generation with equatorward propagation near the tachocline (e.g. Charbonneau and MacGregor 1997; Dikpati and Charbonneau 1999; Dikpati and Gilman 2001). These simulations emphasized that the tachocline is a key physical component in the solar dynamo mechanism. Yet, it is observed that even fully convective M dwarfs without tachoclines exhibit starspots and the so-called magnetic 'activity-rotation correlation' (e.g. Reiners et al. 2014; Wright and Drake 2016; Reiners et al. 2022). Further, some 3D convective dynamo models demonstrate that buoyantly rising magnetic flux structures can be generated within the bulk of the convection zone (see Sect. 3.1). With the recent emphasis on the role that convection plays (both local and mean flows) in active region emergence on the Sun (see also Sect. 4), stars without tachoclines can offer some additional insights into how active-region-scale magnetism is manifested.

The observed diversity in the 3D geometry (i.e. vector components) of stellar photospheric magnetic fields poses another problem for numerical simulations of flux emergence. Zeeman-Doppler imaging of cool stars indicate that the magnetic energy in the toroidal component increases with the poloidal field for more active stars (See et al. 2015). Though with large scatter, the observational relation is steeper than one-to-one scaling for stars with masses above 0.5 $M_{\odot}$, with a power index of 1.25 ± 0.06. The existence of a large amount of toroidal flux on active stars provides valuable constraints for the theory of magnetic flux emergence. Further analysis and interpretation by numerical simulations are needed to understand how such magnetic landscapes occur.

6.2 Modelling the Distribution of Activity on Stars: Hints from Simulations

6.2.1 Active Nests and Longitudes

We noted in Sect. 6.1 that the unsigned surface magnetic flux increases with the rotation rate, for a given effective temperature. Whether this is due to increasing emergence frequency of active regions or larger sizes of individual active regions is unclear. These two scenarios do not exclude each other. An increased tendency for active regions to emerge near existing sites of emergence, known as active nests, is another possibility (Işık et al. 2020, see also van Saders et al. in this volume).

Observations indicate that manifestations of solar activity, including sunspots, coronal flares, and coronal streamers, are distributed inhomogeneously in longitude (e.g. Jetsu et al. 1997; Berdyugina and Usoskin 2003; Li 2011). Some other cool stars and young rapid rotators also exhibit these so-called 'active longitudes' (e.g. Järvinen et al. 2005; García-Alvarez et al. 2011; Luo et al. 2022). The cause of active longitudes is still unknown, but a few theories have been put forward. One simple suggestion is that a long-lived localization of toroidal, amplified magnetic field at the base of the convection zone could spawn the onset of a magnetic buoyancy instability, promoting a series of rising flux loops (e.g. Ruzmaikin 1998). Similarly, the convective dynamo simulations of Nelson et al. (2011, 2013) generate

wreaths of magnetism within the convection zone that spawn buoyant bundles of flux when localized regions exceed a threshold field strength. Although, this effect is perhaps more closely related to the 'active nest' phenomenon described above.

Instead of relying on the localized enhancement of magnetic fields at particular longitudes, Dikpati and Gilman (2005) show that MHD instabilities within a shallow water model of the tachocline can produce simultaneous variations in the tachocline thickness and tipping instabilities of the toroidal magnetic field there. A correlation between a 'bulge' in the tachocline and a tipped toroidal band can force the magnetic field into the convection zone where it will rise buoyantly. Weber et al. (2013a) present yet another alternate theory utilizing their thin flux tube simulations embedded in solar-like convection (Weber et al. 2011, 2013b), which shows that active longitudes might also arise from the presence of rotationally aligned giant-cell convection. The simulations exhibit a pattern of flux emergence with longitudinal modes of low order and low-latitude alignment across the equator. Essentially, the extent of giant-cell upflows and the strong downflow boundaries form windows within which rising flux tubes can emerge. Although, Weber et al. (2013a) use 'active longitudes' to refer to a longitudinal alignment of flux emergence rather than repeated flux emergence at specific longitudes for multiple rotations. In reality, it is likely that both the amplification of localized magnetic fields and the effects of convective flows (which can also amplify localized fields) play a role in the active longitude and active nest phenomena.

Active longitudes have also been observed on stars in close binary systems (e.g. Berdyugina and Tuominen 1998; Berdyugina 2005). In this case tidal forcing was shown to affect the flux emergence patterns, leading to active longitudes on opposite sides of the star (Holzwarth and Schüssler 2003). An exploration of the surface distribution of flux emergence for increasing stellar activity level has now become a necessity for physics-based numerical simulations, to better understand how stellar activity patterns scale with the activity level and the rotation rate.

6.2.2 Emergence Latitudes and Tilts

Although highly simplified, simulations employing the thin flux tube approximation have been used as tools to explore the distribution of magnetic activity on stars with varying rotation rates (Schüssler et al. 1996) and spectral types (Granzer et al. 2000). These models once again point toward the importance of the rotationally-driven Coriolis force on flux tube dynamics (see also Sect. 3.2). The existence of high-latitude and polar spots on stars with more rapid rotation and/or deeper convective envelopes can be explained by angular momentum conservation of a rising flux loop, leading to an internal retrograde flow. In the co-rotating frame, this effect would be experienced as an inward directed Coriolis force component towards the rotation axis, with a magnitude that increasingly dominates the radially outward buoyancy with more rapid rotation (Schüssler and Solanki 1992). The general trend is that beyond four times the solar rotation rate, a zone of avoidance forms around the equator, where no flux emergence occur (Işık et al. 2011, 2018). In these simulations, the initial field strengths of toroidal flux tubes are assumed to be close to the analytical prediction of the onset of magnetic buoyancy instability. This limits the initial field strengths to the range 80-110 kG for the solar model with the initial tube location at the middle of the overshoot region below the convection zone. In a solar-type star rotating eight times faster, the range is in 150-350 kG, so that rotation stabilizes the tubes at a fixed field strength, owing mainly to angular momentum conservation (Işık et al. 2018, see Fig. 2). For rapidly rotating early K dwarfs and subgiants, the equatorial band of avoidance is somewhat widened in latitude, owing simply to the geometry of the convection zone boundaries: when the fractional depth

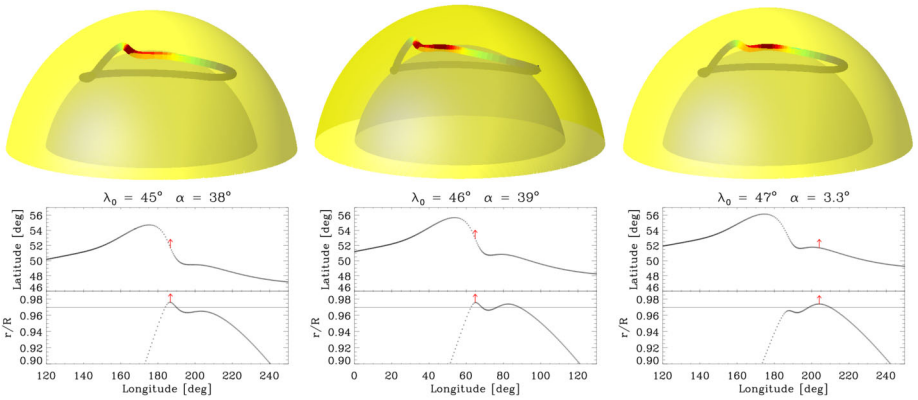

Fig. 5 Geometry of three emerging flux loops with initial latitudes λ_0 at the base of the convection zone and emergence tilt angles α. Upper panels: The parts of the tube that are beneath the outer sphere (0.97 $R_\odot$) are shaded in grey, whereas the emerged parts are brighter. The colours denote the cross-sectional tube radius (the redder the thicker). Lower panels: latitudinal and radial projections of the tubes. The horizontal line on the radial profile corresponds to the location of the outer sphere (0.97 $R_\odot$), where α is measured from footpoint locations. The red arrows denote the apex of each tube. Işık et al., A&A, 620, A177 (2018), reproduced with permission © ESO

of the convection zone increases (ie, towards cooler stars), the poleward-deflected tube apex can emerge at even higher latitudes (Granzer et al. 2000; Işık et al. 2011).

The aforementioned simulations were based on the assumption that active-region producing flux tubes were formed near the base of the convection zone in the overshoot region, in the same way as for the idealized flux tubes in the Sun. It should be noted that in these studies (Işık et al. 2011, 2018), thin flux tubes rise in the presence of a differential rotation profile $\Delta\Omega$, which is kept constant with increasing stellar rotation rate. Taking notes from the simulations of Weber et al. (2011, 2013b), it is likely that incorporating turbulent, time-varying convective flows could modify these trends.

Thin flux tube simulations have also shown that the tilt angles near emergence generally increase with the rotation rate (Işık et al. 2018). This is consistent with the Coriolis acceleration along the tube apex being proportional to the local rotation rate. An increase of the tilt angle limits flux cancellation within the emerged bipolar regions and supports stronger fields to accumulate at the rotational poles (see also Işık et al. 2007).[2] The tilt angles are not only larger in average than solar ones, but their variance is also larger, showing jumps at some emergence latitudes. Such a jump is demonstrated in Fig. 5, which shows the detailed geometry of the flux tube apex starting close to 45° latitude and emerging around 52°. When the initial latitude λ_0 is above 46°, the prograde part of the apex is intruded by a more east-west oriented and broader peak, leading to a tilt angle of about 3°. For $\lambda_0 < 46°$, the large-tilt loop (38°) emerges before the small-tilt loop. Possibly, such multiple-peaked adjacent loops emerge on active stars at certain latitudes, leading to complex active-region topologies with enhanced free energy deposits for the upper atmosphere.

M-dwarfs with masses $\leq$0.35 $M_\odot$ are fully convective, and so lack a tachocline. Yet, in at least some ways, this magnetism is similar to that observed in Sun-like stars (see Sect. 6.1). Weber and Browning (2016) embed the thin flux tube model within simulations of time-

[2]However, with the latitudinal distribution of emerging flux being confined to high latitudes, the stellar dynamo might not be dominated by the dipolar mode.

varying giant-cell convection to explore flux emergence trends in fully convective M dwarfs. Since there is no tachocline layer of shear, they introduce flux tubes at depths of 0.5 $R_\star$ and 0.75 $R_\star$ to sample the differing mean and local time-varying flows at each depth. A range of initial flux tube field strengths of 30-200 kG are chosen. On the lower end (30 kG), this encompasses magnetic fields that would not be too susceptible to suppression of their rise due to turbulent downflows. On the upper end (200 kG), this excludes field strengths above which the flux tubes would rise faster than they could plausibly be generated by large-scale convective eddies (Browning et al. 2016). Convection modulates the flux tubes as they rise, both promoting localized rising loops while suppressing the global rise of flux tubes (akin to magnetic pumping) for those initiated in the deeper interior at lower latitudes (see also Weber et al. 2017). Within these simulations, a robust result is a tendency for flux tubes to rise parallel to the rotation axis (see Sect. 3.2 and the first paragraph in this section), leading to a preference of mid-to-high latitude flux emergence. However, low latitude flux emergence is found in special cases where the flux tubes are initiated closer to the surface and are of strong magnetic fields, or of weaker fields and rise through regions of prograde differential rotation near the equator.

7 Moving Forward

Active regions define the solar cycle, and in some models are an integral part of the transformation of the toroidal field to the poloidal field (Sect. 5). Understanding their origins, formation and distribution will place tight constraints on their role in the solar dynamo and provide insights into these same processes in other cool stars. Typically, active-region-scale magnetism has been modeled as buoyantly rising, fibril tubes originating in the deep interior (Sect. 3.2). New observations and simulations now suggest a shifting paradigm away from these idealized, isolated flux tubes toward a paradigm with a more complex, yet realistic, interplay between rising bundles of magnetism and their surroundings.

Observations of surface magnetism demonstrate that active region flux emergence is a more 'passive' process than was originally thought (Sect. 4). The upward rise of the magnetism as detected near the surface is typical of convective upflows, placing much less of an emphasis on buoyancy in this region. However, it is not yet possible to say whether this influence of convection over buoyancy is confined only to the near-surface regions, or if it extends to the deeper origin of the magnetic structure.

In idealized flux tube simulations, the Coriolis force leads to a geometrical asymmetry in the rising loop legs and a tilting action of these legs toward the equator. The former has been used as an explanation for why the leading active region polarity moves prograde faster than the following polarity moves retrograde. However, it is shown that the east-west motion of active regions is actually symmetric with respect to the local rotation speed which varies with latitude (as described by Snodgrass and Ulrich 1990, see Sect. 4.1). Further, the observed Joy's Law trend may not be consistent with the latitudinally-dependent tilt that the legs of a flux tube acquire as it rises through the convection zone (Sect. 4.3). The examples here and in the previous paragraph are observational constraints that are inconsistent with thin flux-tube models.

No global convective dynamo models have yet been able to produce starspots, partly because they do not include a realistic surface layer. Yet, we know that the surface distribution of emerging flux and the timing of their appearance is a key ingredient in Babcock–Leighton flux-transport dynamo models. Indeed, these incorporate ingredients self-consistently generated in global convective dynamo models such as differential rotation and meridional circulation. Also, they often assume that the primary region of magnetic field generation is

at the tachocline. However, some convective dynamo simulations show that rising bundles of magnetism can be built within the bulk of the convection zone. At present, the exact generation region of active-region-scale magnetism and its strength is unknown. Learning more about the distribution of starspots across stellar photospheres for both Sun-like and fully convective stars may help to better constrain the origin of coherent magnetic structures in the interior. Knowing how the patterns of flux emergence vary as a function of stellar rotation and inferred surface differential rotation will also play a role in disentangling the imprints of rotation, mean flows, and shearing regions on the flux emergence pattern.

To fully understand the extent to which flux emergence is a passive process, more stringent constraints from observations are still needed. But to understand what is happening below the surface, more simulations are critical. In particular, we suggest a strong emphasis to be placed on developing simulations that connect near-surface simulations with deeper flux emergence and dynamo models with fidelity. Further statistical analysis of solar active region emergence properties dependent on, for example, the extremes of magnetic flux and latitude, are also needed.

We conclude with some open questions regarding magnetic flux emergence in the Sun and other cool stars, raised by the observational and theoretical understanding presented, that we anticipate can be addressed in the next decade:

- What properties of active region formation are driven primarily by the influence of convection?
- To what extent do the Coriolis force, convective flows, and tension, twist, and writhe of the magnetic field contribute to the observed Joy's law trend?
- What is the important physics that must be faithfully simulated to capture the observed statistical properties of emerging active regions?
- In our Sun, where is the primary region of generation for active-region-scale magnetism - the tachocline, near-surface, bulk of the convection zone, or some combination of these?
- Can signatures of the underlying dynamo be found in patterns of magnetic activity (as reviewed here) on the photospheres of the Sun and other cool stars?

Appendix 1: Defining the Duration of Active Region Emergence

Here we describe how we computed the duration of the active region emergence process as shown in Fig. 2.

Figure 6 shows the evolution of the mean unsigned magnetic field, $\langle B \rangle$ within the central region of 49 Mm radius the map. The emergence time is defined as being 10% of the total magnetic flux 36 hours after the active region was officially named (see Schunker et al. 2016, for more details). The maps are centred on the flux-weighted centre of the active region about the time of emergence (for a detailed definition see Schunker et al. 2016; Birch et al. 2016) for four example active regions from the Solar Dynamics Observatory Helioseismic Emerging Active Regions survey (SDO/HEARS) (Schunker et al. 2016) which contains a total of 180 active regions.

The emergence of an active region ends when all of the magnetic field has appeared at the surface. We identified the time when the mean line-of-sight unsigned magnetic field $\langle B \rangle$ with a 5.3 hour cadence was a maximum. If the maximum occurred within three time intervals ($\approx$16 hours) of the end of the time series it is difficult to assess whether it is still emerging (e.g. AR11103 in Fig. 6), and so we exclude these regions (35 in total). Otherwise, we fit a quadratic to the $\langle B \rangle$ values between 8 hours (two time intervals) before and 13 hours (three time intervals) after the time when the maximum mean magnetic field $\langle B \rangle_{\max}$

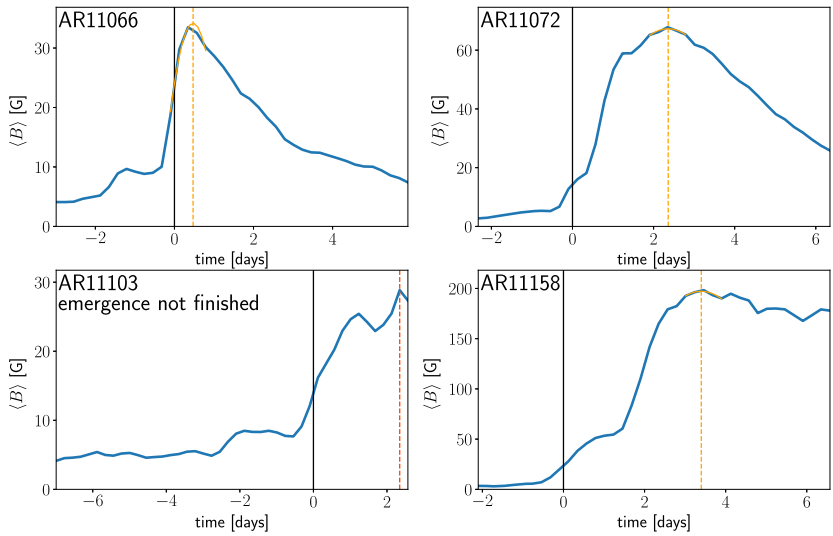

Fig. 6 Examples of the evolution of the averaged unsigned magnetic field within the central 49 Mm radius, $\langle B \rangle$, for four emerging active regions relative to the emergence time (blue). For AR11066, AR11072 and AR11158 the orange curve shows the least-squares fit of a quadratic to the peak of the curve and the dashed vertical line shows the time of the maximum value of the quadratic. Since the maximum value of $\langle B \rangle$ for AR11103 occurs within the last 16 hours of the time series, we exclude it from our sample

occurred, and we defined the time of the maximum of the quadratic function as the end time of the emergence process. There is no physical basis for fitting a quadratic, only that we found it fit the peak reasonably well (see Fig. 6). The duration of the emergence process is the difference between end of the emergence process and the emergence time.

List of 120 NOAA active region numbers included in Fig. 3: 11066, 11070, 11072, 11075, 11076, 11079, 11081, 11086, 11088, 11103, 11105, 11114, 11122, 11132, 11136, 11137, 11138, 11141, 11142, 11145, 11148, 11154, 11158, 11159, 11167, 11198, 11199, 11200, 11206, 11209, 11211, 11214, 11223, 11239, 11273, 11288, 11290, 11297, 11300, 11304, 11310, 11322, 11327, 11331, 11381, 11397, 11400, 11404, 11406, 11414, 11416, 11431, 11437, 11446, 11450, 11456, 11472, 11497, 11500, 11510, 11511, 11523, 11531, 11547, 11549, 11551, 11554, 11565, 11570, 11574, 11597, 11603, 11607, 11624, 11626, 11627, 11631, 11640, 11645, 11686, 11696, 11699, 11703, 11707, 11712, 11718, 11736, 11750, 11780, 11781, 11784, 11786, 11789, 11807, 11813, 11821, 11824, 11833, 11843, 11855, 11867, 11874, 11878, 11886, 11894, 11915, 11924, 11946, 11962, 11969, 11978, 11992, 12003, 12011, 12039, 12064, 12078, 12099, 12118, 12119.

Acknowledgements HS is the recipient of an Australian Research Council Future Fellowship Award (project number FT220100330) funded by the Australian Government and her contribution is partially funded by this grant. LJ acknowledges funding by the Institut Universitaire de France. The authors thank the reviewers for their comments, which improved the clarity of this manuscript.

Author Contribution All authors contributed equally to this work.

Funding Open Access funding enabled and organized by Projekt DEAL.

Declarations

Competing Interests The authors have no conflicts of interest to declare that are relevant to the content of this article.

References

Abbett WP, Fisher GH, Fan Y (2001) The effects of rotation on the evolution of rising omega loops in a stratified model convection zone. Astrophys J 546(2):1194–1203. https://doi.org/10.1086/318320. arXiv:astro-ph/0008501 [astro-ph]

Archontis V, Hood AW (2010) Flux emergence and coronal eruption. Astron Astrophys 514:A56. https://doi.org/10.1051/0004-6361/200913502. arXiv:1003.2333 [astro-ph.SR]

Augustson K, Brun AS, Miesch M et al (2015) Grand minima and equatorward propagation in a cycling stellar convective dynamo. Astrophys J 809(2):149. https://doi.org/10.1088/0004-637X/809/2/149. arXiv:1410.6547 [astro-ph.SR]

Babcock HW (1961) The topology of the Sun's magnetic field and the 22-year cycle. Astrophys J 133:572. https://doi.org/10.1086/147060

Baldner CS, Basu S (2008) Solar cycle related changes at the base of the convection zone. Astrophys J 686(2):1349–1361. https://doi.org/10.1086/591514. arXiv:0807.0442 [astro-ph]

Barnes JR, Collier Cameron A, Unruh YC et al (1998) Latitude distributions and lifetimes of star-spots on G dwarfs in the α Persei cluster. Mon Not R Astron Soc 299(3):904–920. https://doi.org/10.1046/j.1365-8711.1998.01805.x

Barnes G, Birch AC, Leka KD et al (2014) Helioseismology of pre-emerging active regions. III. Statistical analysis. Astrophys J 786:19. https://doi.org/10.1088/0004-637X/786/1/19. arXiv:1307.1938 [astro-ph.SR]

Barnes JR, Jeffers SV, Jones HRA et al (2015) Starspot distributions on fully convective M dwarfs: implications for radial velocity planet searches. Astrophys J 812(1):42. https://doi.org/10.1088/0004-637X/812/1/42. arXiv:1509.05284 [astro-ph.SR]

Baumgartner C, Birch AC, Schunker H et al (2022) Impact of spatially correlated fluctuations in sunspots on metrics related to magnetic twist. Astron Astrophys 664:A183. https://doi.org/10.1051/0004-6361/202243357. arXiv:2207.02135 [astro-ph.SR]

Bekki Y, Cameron RH (2023) Three-dimensional non-kinematic simulation of the post-emergence evolution of bipolar magnetic regions and the Babcock-Leighton dynamo of the Sun. Astron Astrophys 670:A101. https://doi.org/10.1051/0004-6361/202244990. arXiv:2209.08178 [astro-ph.SR]

Berdyugina SV (2005) Starspots: a key to the stellar dynamo. Living Rev Sol Phys 2(1):8. https://doi.org/10.12942/lrsp-2005-8

Berdyugina SV, Tuominen I (1998) Permanent active longitudes and activity cycles on RS CVn stars. Astron Astrophys 336:L25–L28

Berdyugina SV, Usoskin IG (2003) Active longitudes in sunspot activity: century scale persistence. Astron Astrophys 405:1121–1128. https://doi.org/10.1051/0004-6361:20030748

Berger MA, Field GB (1984) The topological properties of magnetic helicity. J Fluid Mech 147:133–148. https://doi.org/10.1017/S0022112084002019

Bice CP, Toomre J (2022) Longitudinally modulated dynamo action in simulated M-dwarf stars. Astrophys J 928(1):51. https://doi.org/10.3847/1538-4357/ac4be0. arXiv:2202.02869 [astro-ph.SR]

Birch AC, Braun DC, Leka KD et al (2013) Helioseismology of pre-emerging active regions. II. Average emergence properties. Astrophys J 762(2):131. https://doi.org/10.1088/0004-637X/762/2/131. arXiv:1303.1391 [astro-ph.SR]

Birch AC, Schunker H, Braun DC et al (2016) A low upper limit on the subsurface rise speed of solar active regions. Sci Adv 2(7):e1600557. https://doi.org/10.1126/sciadv.1600557. arXiv:1607.05250 [astro-ph.SR]

Birch AC, Schunker H, Braun DC et al (2019) Average surface flows before the formation of solar active regions and their relationship to the supergranulation pattern. Astron Astrophys 628:A37. https://doi.org/10.1051/0004-6361/201935591

Brandenburg A, Kleeorin N, Rogachevskii I (2013) Self-assembly of shallow magnetic spots through strongly stratified turbulence. Astrophys J Lett 776(2):L23. https://doi.org/10.1088/2041-8205/776/2/L23. arXiv:1306.4915 [astro-ph.SR]

Brown BP, Miesch MS, Browning MK et al (2011) Magnetic cycles in a convective dynamo simulation of a young solar-type star. Astrophys J 731(1):69. https://doi.org/10.1088/0004-637X/731/1/69. arXiv:1102.1993 [astro-ph.SR]

Browning MK, Weber MA, Chabrier G et al (2016) Theoretical limits on magnetic field strengths in low-mass stars. Astrophys J 818(2):189. https://doi.org/10.3847/0004-637X/818/2/189. arXiv:1512.05692 [astro-ph.SR]

Brun AS, Browning MK (2017) Magnetism, dynamo action and the solar-stellar connection. Living Rev Sol Phys 14(1):4. https://doi.org/10.1007/s41116-017-0007-8

Caligari P, Moreno-Insertis F, Schussler M (1995) Emerging flux tubes in the solar convection zone. I. Asymmetry, tilt, and emergence latitude. Astrophys J 441:886. https://doi.org/10.1086/175410

Cameron RH, Schüssler M (2012) Are the strengths of solar cycles determined by converging flows towards the activity belts? Astron Astrophys 548:A57. https://doi.org/10.1051/0004-6361/201219914. arXiv:1210.7644 [astro-ph.SR]

Cameron R, Schüssler M (2015) The crucial role of surface magnetic fields for the solar dynamo. Science 347(6228):1333–1335. https://doi.org/10.1126/science.1261470. arXiv:1503.08469 [astro-ph.SR]

Cameron RH, Jiang J, Schmitt D et al (2010) Surface flux transport modeling for solar cycles 15-21: effects of cycle-dependent tilt angles of sunspot groups. Astrophys J 719(1):264–270. https://doi.org/10.1088/0004-637X/719/1/264. arXiv:1006.3061 [astro-ph.SR]

Cameron RH, Duvall TL, Schüssler M et al (2018) Observing and modeling the poloidal and toroidal fields of the solar dynamo. Astron Astrophys 609:A56. https://doi.org/10.1051/0004-6361/201731481. arXiv:1710.07126 [astro-ph.SR]

Castenmiller MJM, Zwaan C, van der Zalm EBJ (1986) Sunspot nests - manifestations of sequences in magnetic activity. Sol Phys 105(2):237–255. https://doi.org/10.1007/BF00172045

Cattaneo F, Hughes DW (1988) The nonlinear breakup of a magnetic layer - instability to interchange modes. J Fluid Mech 196:323–344. https://doi.org/10.1017/S0022112088002721

Charbonneau P, MacGregor KB (1997) Solar interface dynamos. II. Linear, kinematic models in spherical geometry. Astrophys J 486(1):502–520. https://doi.org/10.1086/304485

Chen F, Rempel M, Fan Y (2017) Emergence of magnetic flux generated in a solar convective dynamo. I. The formation of sunspots and active regions, and the origin of their asymmetries. Astrophys J 846(2):149. https://doi.org/10.3847/1538-4357/aa85a0. arXiv:1704.05999 [astro-ph.SR]

Cheung MCM, Isobe H (2014) Flux emergence (theory). Living Rev Sol Phys 11(1):3. https://doi.org/10.12942/lrsp-2014-3

Cheung MCM, Rempel M, Title AM et al (2010) Simulation of the formation of a solar active region. Astrophys J 720(1):233–244. https://doi.org/10.1088/0004-637X/720/1/233. arXiv:1006.4117 [astro-ph.SR]

Cheung MCM, van Driel-Gesztelyi L, Martínez Pillet V et al (2017) The life cycle of active region magnetic fields. Space Sci Rev 210(1–4):317–349. https://doi.org/10.1007/s11214-016-0259-y

Chou DY, Wang H (1987) The separation velocity of emerging magnetic flux. Sol Phys 110(1):81–99. https://doi.org/10.1007/BF00148204

Choudhuri AR, Gilman PA (1987) The influence of the Coriolis force on flux tubes rising through the solar convection zone. Astrophys J 316:788. https://doi.org/10.1086/165243

Cline KS, Brummell NH, Cattaneo F (2003) Dynamo action driven by shear and magnetic buoyancy. Astrophys J 599(2):1449–1468. https://doi.org/10.1086/379366

Dasi-Espuig M, Solanki SK, Krivova NA et al (2010) Sunspot group tilt angles and the strength of the solar cycle. Astron Astrophys 518:A7. https://doi.org/10.1051/0004-6361/201014301. arXiv:1005.1774 [astro-ph.SR]

Davenport JRA, Hebb L, Hawley SL (2015) Detecting differential rotation and starspot evolution on the M dwarf GJ 1243 with Kepler. Astrophys J 806(2):212. https://doi.org/10.1088/0004-637X/806/2/212. arXiv:1505.01524 [astro-ph.SR]

Dikpati M, Charbonneau P (1999) A Babcock-Leighton flux transport dynamo with solar-like differential rotation. Astrophys J 518(1):508–520. https://doi.org/10.1086/307269

Dikpati M, Gilman PA (2001) Flux-transport dynamos with α-effect from global instability of tachocline differential rotation: a solution for magnetic parity selection in the Sun. Astrophys J 559(1):428–442. https://doi.org/10.1086/322410

Dikpati M, Gilman PA (2005) A shallow-water theory for the Sun's active longitudes. Astrophys J Lett 635(2):L193–L196. https://doi.org/10.1086/499626

D'Silva S, Choudhuri AR (1993) A theoretical model for tilts of bipolar magnetic regions. Astron Astrophys 272:621
Emonet T, Moreno-Insertis F (1998) The physics of twisted magnetic tubes rising in a stratified medium: two-dimensional results. Astrophys J 492(2):804–821. https://doi.org/10.1086/305074. arXiv:astro-ph/9711043 [astro-ph]
Fan Y (2001) Nonlinear growth of the three-dimensional undular instability of a horizontal magnetic layer and the formation of arching flux tubes. Astrophys J 546(1):509–527. https://doi.org/10.1086/318222
Fan Y (2008) The three-dimensional evolution of buoyant magnetic flux tubes in a model solar convective envelope. Astrophys J 676(1):680–697. https://doi.org/10.1086/527317
Fan Y (2021) Magnetic fields in the solar convection zone. Living Rev Sol Phys 18(1):5. https://doi.org/10.1007/s41116-021-00031-2
Fan Y, Fang F (2014) A simulation of convective dynamo in the solar convective envelope: maintenance of the solar-like differential rotation and emerging flux. Astrophys J 789(1):35. https://doi.org/10.1088/0004-637X/789/1/35. arXiv:1405.3926 [astro-ph.SR]
Fan Y, Gong D (2000) On the twist of emerging flux loops in the solar convection zone. Sol Phys 192:141–157. https://doi.org/10.1023/A:1005260207672
Fan Y, Fisher GH, Deluca EE (1993) The origin of morphological asymmetries in bipolar active regions. Astrophys J 405:390. https://doi.org/10.1086/172370
Fan Y, Fisher GH, McClymont AN (1994) Dynamics of emerging active region flux loops. Astrophys J 436:907. https://doi.org/10.1086/174967
Fan Y, Zweibel EG, Lantz SR (1998) Two-dimensional simulations of buoyantly rising, interacting magnetic flux tubes. Astrophys J 493(1):480–493. https://doi.org/10.1086/305122
Fan Y, Abbett WP, Fisher GH (2003) The dynamic evolution of twisted magnetic flux tubes in a three-dimensional convecting flow. I. Uniformly buoyant horizontal tubes. Astrophys J 582(2):1206–1219. https://doi.org/10.1086/344798
Favier B, Jouve L, Edmunds W et al (2012) How can large-scale twisted magnetic structures naturally emerge from buoyancy instabilities? Mon Not R Astron Soc 426(4):3349–3359. https://doi.org/10.1111/j.1365-2966.2012.21920.x. arXiv:1208.4787 [astro-ph.SR]
Ferriz-Mas A, Schüssler M (1995) Instabilities of magnetic flux tubes in a stellar convection zone II. Flux rings outside the equatorial plane. Geophys Astrophys Fluid Dyn 81(3):233–265. https://doi.org/10.1080/03091929508229066
Fuentes ML, Démoulin P, Mandrini CH et al (2003) Magnetic twist and writhe of active regions. On the origin of deformed flux tubes. Astron Astrophys 397:305–318. https://doi.org/10.1051/0004-6361:20021487. arXiv:1411.5626 [astro-ph.SR]
García RA, Mathur S, Salabert D et al (2010) CoRoT reveals a magnetic activity cycle in a Sun-like star. Science 329(5995):1032. https://doi.org/10.1126/science.1191064. arXiv:1008.4399 [astro-ph.SR]
García-Alvarez D, Lanza AF, Messina S et al (2011) Starspots on the fastest rotators in the β Pictoris moving group. Astron Astrophys 533:A30. https://doi.org/10.1051/0004-6361/201116646. arXiv:1107.5688 [astro-ph.SR]
Ghizaru M, Charbonneau P, Smolarkiewicz PK (2010) Magnetic cycles in global large-eddy simulations of solar convection. Astrophys J Lett 715(2):L133–L137. https://doi.org/10.1088/2041-8205/715/2/L133
Gilman PA, Howard R (1985) Rotation rates of leader and follower sunspots. Astrophys J 295:233–240. https://doi.org/10.1086/163368
Gizon L, Cameron RH, Pourabdian M et al (2020) Meridional flow in the Sun's convection zone is a single cell in each hemisphere. Science 368(6498):1469–1472. https://doi.org/10.1126/science.aaz7119
Granzer T, Schüssler M, Caligari P et al (2000) Distribution of starspots on cool stars. II. Pre-main-sequence and ZAMS stars between 0.4 $M_\odot$ and 1.7 $M_\odot$. Astron Astrophys 355:1087–1097
Hale GE, Ellerman F, Nicholson SB et al (1919) The magnetic polarity of Sun-spots. Astrophys J 49:153. https://doi.org/10.1086/142452
Harvey KL (1993) Magnetic bipoles on the Sun. PhD thesis. Utrecht University
Hazra G, Nandy D, Kitchatinov L et al (2023) Mean field models of flux transport dynamo and meridional circulation in the Sun and stars. Space Sci Rev 219:39. https://doi.org/10.1007/s11214-023-00982-y arXiv:2302.09390 [astro-ph.SR]
Holzwarth V, Schüssler M (2003) Dynamics of magnetic flux tubes in close binary stars. II. Nonlinear evolution and surface distributions. Astron Astrophys 405:303–311. https://doi.org/10.1051/0004-6361:20030584. arXiv:astro-ph/0304498 [astro-ph]
Hotta H, Iijima H (2020) On rising magnetic flux tube and formation of sunspots in a deep domain. Mon Not R Astron Soc 494(2):2523–2537. https://doi.org/10.1093/mnras/staa844. arXiv:2003.10583 [astro-ph.SR]
Hotta H, Rempel M, Yokoyama T (2016) Large-scale magnetic fields at high Reynolds numbers in magneto-hydrodynamic simulations. Science 351(6280):1427–1430. https://doi.org/10.1126/science.aad1893

Howard RF (1996) Axial tilt angles of active regions. Sol Phys 169(2):293–301. https://doi.org/10.1007/BF00190606

Işık E (2015) A mechanism for the dependence of sunspot group tilt angles on cycle strength. Astrophys J Lett 813(1):L13. https://doi.org/10.1088/2041-8205/813/1/L13. arXiv:1510.04323 [astro-ph.SR]

Işık E, Schüssler M, Solanki SK (2007) Magnetic flux transport on active cool stars and starspot lifetimes. Astron Astrophys 464(3):1049–1057. https://doi.org/10.1051/0004-6361:20066623. arXiv:astro-ph/0612399 [astro-ph]

Işık E, Schmitt D, Schüssler M (2011) Magnetic flux generation and transport in cool stars. Astron Astrophys 528:A135. https://doi.org/10.1051/0004-6361/201014501. arXiv:1102.0569 [astro-ph.SR]

Işık E, Solanki SK, Krivova NA et al (2018) Forward modelling of brightness variations in Sun-like stars. I. Emergence and surface transport of magnetic flux. Astron Astrophys 620:A177. https://doi.org/10.1051/0004-6361/201833393. arXiv:1810.06728 [astro-ph.SR]

Işık E, Shapiro AI, Solanki SK et al (2020) Amplification of brightness variability by active-region nesting in solar-like stars. Astrophys J Lett 901(1):L12. https://doi.org/10.3847/2041-8213/abb409. arXiv:2009.00692 [astro-ph.SR]

Järvinen SP, Berdyugina SV, Tuominen I et al (2005) Magnetic activity in the young solar analog AB Dor. Active longitudes and cycles from long-term photometry. Astron Astrophys 432(2):657–664. https://doi.org/10.1051/0004-6361:20041998

Jeffers SV, Barnes JR, Collier Cameron A (2002) The latitude distribution of star-spots on He 699. Mon Not R Astron Soc 331(3):666–672. https://doi.org/10.1046/j.1365-8711.2002.05143.x

Jeffers SV, Cameron RH, Marsden SC et al (2022) The crucial role of surface magnetic fields for stellar dynamos: ϵ Eridani, 61 Cygni A, and the Sun. Astron Astrophys 661:A152. https://doi.org/10.1051/0004-6361/202142202. arXiv:2201.07530 [astro-ph.SR]

Jetsu L, Pohjolainen S, Pelt J et al (1997) Is the longitudinal distribution of solar flares nonuniform? Astron Astrophys 318:293–307

Jha BK, Karak BB, Mandal S et al (2020) Magnetic field dependence of bipolar magnetic region tilts on the Sun: indication of tilt quenching. Astrophys J Lett 889(1):L19. https://doi.org/10.3847/2041-8213/ab665c. arXiv:1912.13223 [astro-ph.SR]

Jiang J, Işik E, Cameron RH et al (2010) The effect of activity-related meridional flow modulation on the strength of the solar polar magnetic field. Astrophys J 717(1):597–602. https://doi.org/10.1088/0004-637X/717/1/597. arXiv:1005.5317 [astro-ph.SR]

Jiao Q, Jiang J, Wang ZF (2021) Sunspot tilt angles revisited: dependence on the solar cycle strength. Astron Astrophys 653:A27. https://doi.org/10.1051/0004-6361/202141215. arXiv:2106.11615 [astro-ph.SR]

Jouve L, Brun AS (2009) Three-dimensional nonlinear evolution of a magnetic flux tube in a spherical shell: influence of turbulent convection and associated mean flows. Astrophys J 701(2):1300–1322. https://doi.org/10.1088/0004-637X/701/2/1300. arXiv:0907.2131 [astro-ph.SR]

Jouve L, Proctor MRE, Lesur G (2010) Buoyancy-induced time delays in Babcock-Leighton flux-transport dynamo models. Astron Astrophys 519:A68. https://doi.org/10.1051/0004-6361/201014455. arXiv:1005.2283 [astro-ph.SR]

Jouve L, Brun AS, Aulanier G (2013) Global dynamics of subsurface solar active regions. Astrophys J 762(1):4. https://doi.org/10.1088/0004-637X/762/1/4. arXiv:1211.7251 [astro-ph.SR]

Jouve L, Brun AS, Aulanier G (2018) Interactions of twisted Ω-loops in a model solar convection zone. Astrophys J 857(2):83. https://doi.org/10.3847/1538-4357/aab5b6. arXiv:1803.04709 [astro-ph.SR]

Käpylä PJ, Mantere MJ, Brandenburg A (2012) Cyclic magnetic activity due to turbulent convection in spherical wedge geometry. Astrophys J Lett 755(1):L22. https://doi.org/10.1088/2041-8205/755/1/L22. arXiv:1205.4719 [astro-ph.SR]

Käpylä PJ, Brandenburg A, Kleeorin N et al (2016) Magnetic flux concentrations from turbulent stratified convection. Astron Astrophys 588:A150. https://doi.org/10.1051/0004-6361/201527731. arXiv:1511.03718 [astro-ph.SR]

Karak BB, Miesch M (2017) Solar cycle variability induced by tilt angle scatter in a Babcock-Leighton solar dynamo model. Astrophys J 847(1):69. https://doi.org/10.3847/1538-4357/aa8636. arXiv:1706.08933 [astro-ph.SR]

Komm R, Morita S, Howe R et al (2008) Emerging active regions studied with ring-diagram analysis. Astrophys J 672:1254–1265. https://doi.org/10.1086/523998

Kosovichev AG, Stenflo JO (2008) Tilt of emerging bipolar magnetic regions on the Sun. Astrophys J Lett 688:L115. https://doi.org/10.1086/595619

Kumar R, Jouve L, Nandy D (2019) A 3D kinematic Babcock Leighton solar dynamo model sustained by dynamic magnetic buoyancy and flux transport processes. Astron Astrophys 623:A54. https://doi.org/10.1051/0004-6361/201834705. arXiv:1901.04251 [astro-ph.SR]

Leighton RB (1969) A magneto-kinematic model of the solar cycle. Astrophys J 156:1. https://doi.org/10.1086/149943

Leka KD, Barnes G, Birch AC et al (2013) Helioseismology of pre-emerging active regions. I. Overview, data, and target selection criteria. Astrophys J 762:130. https://doi.org/10.1088/0004-637X/762/2/130. arXiv:1303.1433 [astro-ph.SR]
Li J (2011) Active longitudes revealed by large-scale and long-lived coronal streamers. Astrophys J 735(2):130. https://doi.org/10.1088/0004-637X/735/2/130. arXiv:1104.5537 [astro-ph.SR]
Linton MG, Dahlburg RB, Antiochos SK (2001) Reconnection of twisted flux tubes as a function of contact angle. Astrophys J 553(2):905–921. https://doi.org/10.1086/320974
Longcope DW, Klapper I (1997) Dynamics of a thin twisted flux tube. Astrophys J 488(1):443–453. https://doi.org/10.1086/304680
Longcope DW, Fisher GH, Pevtsov AA (1998) Flux-tube twist resulting from helical turbulence: the Σ-effect. Astrophys J 507(1):417–432. https://doi.org/10.1086/306312
López Fuentes MC, Demoulin P, Mandrini CH et al (2000) The counterkink rotation of a non-hale active region. Astrophys J 544(1):540–549. https://doi.org/10.1086/317180. arXiv:1412.1456 [astro-ph.SR]
Luo X, Gu S, Xiang Y et al (2022) Active longitudes and starspot evolution of the young rapidly rotating star USNO-B1.0 1388-0463685 discovered in the Yunnan-Hong Kong survey. Mon Not R Astron Soc 514(1):1511–1521. https://doi.org/10.1093/mnras/stac1406
Luoni ML, Démoulin P, Mandrini CH et al (2011) Twisted flux tube emergence evidenced in longitudinal magnetograms: magnetic tongues. Sol Phys 270(1):45. https://doi.org/10.1007/s11207-011-9731-8
Manek B, Brummell N (2021) On the origin of solar hemispherical helicity rules: simulations of the rise of magnetic flux concentrations in a background field. Astrophys J 909(1):72. https://doi.org/10.3847/1538-4357/abd859. arXiv:2101.03472 [astro-ph.SR]
Manek B, Brummell N, Lee D (2018) The rise of a magnetic flux tube in a background field: solar helicity selection rules. Astrophys J Lett 859(2):L27. https://doi.org/10.3847/2041-8213/aac723. arXiv:1805.08806 [astro-ph.SR]
Manek B, Pontin C, Brummell N (2022) The rise of buoyant magnetic structures through convection with a background magnetic field. Astrophys J 929(2):162. https://doi.org/10.3847/1538-4357/ac5828. arXiv:2204.13078 [astro-ph.SR]
Martínez-Sykora J, Moreno-Insertis F, Cheung MCM (2015) Multi-parametric study of rising 3D buoyant flux tubes in an adiabatic stratification using AMR. Astrophys J 814(1):2. https://doi.org/10.1088/0004-637X/814/1/2. arXiv:1507.01506 [astro-ph.SR]
Matilsky LI, Toomre J (2020) Exploring bistability in the cycles of the solar dynamo through global simulations. Astrophys J 892(2):106. https://doi.org/10.3847/1538-4357/ab791c. arXiv:1912.08158 [astro-ph.SR]
Matthews PC, Hughes DW, Proctor MRE (1995) Magnetic buoyancy, vorticity, and three-dimensional flux-tube formation. Astrophys J 448:938. https://doi.org/10.1086/176022
McClintock BH, Norton AA (2016) Tilt angle and footpoint separation of small and large bipolar sunspot regions observed with HMI. Astrophys J 818:7. https://doi.org/10.3847/0004-637X/818/1/7
Miesch MS, Dikpati M (2014) A three-dimensional Babcock-Leighton solar dynamo model. Astrophys J Lett 785(1):L8. https://doi.org/10.1088/2041-8205/785/1/L8. arXiv:1401.6557 [astro-ph.SR]
Moreno-Insertis F, Emonet T (1996) The rise of twisted magnetic tubes in a stratified medium. Astrophys J Lett 472:L53. https://doi.org/10.1086/310360
Moreno-Insertis F, Schüssler M, Ferriz-Mas A (1992) Storage of magnetic flux tubes in a convective overshoot region. Astron Astrophys 264(2):686–700
Moreno-Insertis F, Caligari P, Schüssler M (1994) Active region asymmetry as a result of the rise of magnetic flux tubes. Sol Phys 153(1–2):449–452. https://doi.org/10.1007/BF00712518
Nagy M, Lemerle A, Labonville F et al (2017) The effect of "rogue" active regions on the solar cycle. Sol Phys 292(11):167. https://doi.org/10.1007/s11207-017-1194-0. arXiv:1712.02185 [astro-ph.SR]
Nandy D (2021) Progress in solar cycle predictions: sunspot cycles 24-25 in perspective. Sol Phys 296(3):54. https://doi.org/10.1007/s11207-021-01797-2. arXiv:2009.01908 [astro-ph.SR]
Nelson NJ, Brown BP, Brun AS et al (2011) Buoyant magnetic loops in a global dynamo simulation of a young Sun. Astrophys J Lett 739(2):L38. https://doi.org/10.1088/2041-8205/739/2/L38. arXiv:1108.4697 [astro-ph.SR]
Nelson NJ, Brown BP, Brun AS et al (2013) Magnetic wreaths and cycles in convective dynamos. Astrophys J 762(2):73. https://doi.org/10.1088/0004-637X/762/2/73. arXiv:1211.3129 [astro-ph.SR]
Nelson NJ, Brown BP, Sacha Brun A et al (2014) Buoyant magnetic loops generated by global convective dynamo action. Sol Phys 289(2):441–458. https://doi.org/10.1007/s11207-012-0221-4. arXiv:1212.5612 [astro-ph.SR]
Parker EN (1955) The formation of sunspots from the solar toroidal field. Astrophys J 121:491. https://doi.org/10.1086/146010
Parker EN (1975) The generation of magnetic fields in astrophysical bodies. X. Magnetic buoyancy and the solar dynamo. Astrophys J 198:205–209. https://doi.org/10.1086/153593

Pevtsov AA, Canfield RC, Latushko SM (2001) Hemispheric helicity trend for solar cycle 23. Astrophys J Lett 549(2):L261–L263. https://doi.org/10.1086/319179
Pevtsov AA, Maleev VM, Longcope DW (2003) Helicity evolution in emerging active regions. Astrophys J 593(2):1217–1225. https://doi.org/10.1086/376733
Pevtsov AA, Berger MA, Nindos A et al (2014) Magnetic helicity, tilt, and twist. Space Sci Rev 186(1–4):285–324. https://doi.org/10.1007/s11214-014-0082-2
Pinto RF, Brun AS (2013) Flux emergence in a magnetized convection zone. Astrophys J 772(1):55. https://doi.org/10.1088/0004-637X/772/1/55. arXiv:1305.2159 [astro-ph.SR]
Pipin VV (2022) On the effect of surface bipolar magnetic regions on the convection zone dynamo. Mon Not R Astron Soc 514(1):1522–1534. https://doi.org/10.1093/mnras/stac1434. arXiv:2112.09460 [astro-ph.SR]
Poisson M, Démoulin P, Mandrini CH et al (2020) Active-region tilt angles from white-light images and magnetograms: the role of magnetic tongues. Astrophys J 894(2):131. https://doi.org/10.3847/1538-4357/ab8944. arXiv:2004.07345 [astro-ph.SR]
Poisson M, Grings F, Mandrini CH et al (2022) Bayesian approach for modeling global magnetic parameters for the solar active region. Astron Astrophys 665:A101. https://doi.org/10.1051/0004-6361/202244058
Prabhu A, Brandenburg A, Käpylä MJ et al (2020) Helicity proxies from linear polarisation of solar active regions. Astron Astrophys 641:A46. https://doi.org/10.1051/0004-6361/202037614. arXiv:2001.10884 [astro-ph.SR]
Reiners A, Schüssler M, Passegger VM (2014) Generalized investigation of the rotation-activity relation: favoring rotation period instead of Rossby number. Astrophys J 794(2):144. https://doi.org/10.1088/0004-637X/794/2/144. arXiv:1408.6175 [astro-ph.SR]
Reiners A, Shulyak D, Käpylä PJ et al (2022) Magnetism, rotation, and nonthermal emission in cool stars. Average magnetic field measurements in 292 M dwarfs. Astron Astrophys 662:A41. https://doi.org/10.1051/0004-6361/202243251. arXiv:2204.00342 [astro-ph.SR]
Rempel M (2003) Thermal properties of magnetic flux tubes. II. Storage of flux in the solar overshoot region. Astron Astrophys 397:1097–1107. https://doi.org/10.1051/0004-6361:20021594
Ruzmaikin A (1998) Clustering of emerging magnetic flux. Sol Phys 181(1):1–12. https://doi.org/10.1023/A:1016563632058
Scherrer PH, Schou J, Bush RI et al (2012) The Helioseismic and Magnetic Imager (HMI) investigation for the Solar Dynamics Observatory (SDO). Sol Phys 275(1–2):207–227. https://doi.org/10.1007/s11207-011-9834-2
Schrijver CJ, Zwaan C (2000) Solar and stellar magnetic activity. Cambridge University Press, Cambridge. https://doi.org/10.1017/CBO9780511546037
Schunker H, Braun DC, Birch AC et al (2016) SDO/HMI survey of emerging active regions for helioseismology. Astron Astrophys 595:A107. https://doi.org/10.1051/0004-6361/201628388. arXiv:1608.08005 [astro-ph.SR]
Schunker H, Birch AC, Cameron RH et al (2019) Average motion of emerging solar active region polarities. I. Two phases of emergence. Astron Astrophys 625:A53. https://doi.org/10.1051/0004-6361/201834627. arXiv:1903.11839 [astro-ph.SR]
Schunker H, Baumgartner C, Birch AC et al (2020) Average motion of emerging solar active region polarities. II. Joy's law. Astron Astrophys 640:A116. https://doi.org/10.1051/0004-6361/201937322. arXiv:2006.05565 [astro-ph.SR]
Schüssler M, Solanki SK (1992) Why rapid rotators have polar spots. Astron Astrophys 264:L13–L16
Schüssler M, Caligari P, Ferriz-Mas A et al (1996) Distribution of starspots on cool stars. I. Young and main sequence stars of 1 $M_{\odot}$. Astron Astrophys 314:503–512
See V, Jardine M, Vidotto AA et al (2015) The energy budget of stellar magnetic fields. Mon Not R Astron Soc 453(4):4301–4310. https://doi.org/10.1093/mnras/stv1925. arXiv:1508.01403 [astro-ph.SR]
See V, Jardine M, Vidotto AA et al (2016) The connection between stellar activity cycles and magnetic field topology. Mon Not R Astron Soc 462(4):4442–4450. https://doi.org/10.1093/mnras/stw2010. arXiv:1610.03737 [astro-ph.SR]
Snodgrass HB, Ulrich RK (1990) Rotation of Doppler features in the solar photosphere. Astrophys J 351:309. https://doi.org/10.1086/168467
Solanki SK (2003) Sunspots: an overview. Astron Astrophys Rev 11(2–3):153–286. https://doi.org/10.1007/s00159-003-0018-4
Spruit HC (1981) Motion of magnetic flux tubes in the solar convection zone and chromosphere. Astron Astrophys 98:155–160
Spruit HC, van Ballegooijen AA (1982) Stability of toroidal flux tubes in stars. Astron Astrophys 106(1):58–66
Spruit HC, van Vallegooijen AA (1982) Erratum - stability of toroidal flux tubes in stars. Astron Astrophys 113:350

Stein RF, Nordlund Å (2012) On the formation of active regions. Astrophys J Lett 753(1):L13. https://doi.org/10.1088/2041-8205/753/1/L13. arXiv:1207.4248 [astro-ph.SR]
Stenflo JO, Kosovichev AG (2012) Bipolar magnetic regions on the Sun: global analysis of the SOHO/MDI data set. Astrophys J 745:129. https://doi.org/10.1088/0004-637X/745/2/129. arXiv:1112.5226 [astro-ph.SR]
Strassmeier KG (2009) Starspots. Astron Astrophys Rev 17(3):251–308. https://doi.org/10.1007/s00159-009-0020-6
Strugarek A, Beaudoin P, Charbonneau P et al (2017) Reconciling solar and stellar magnetic cycles with nonlinear dynamo simulations. Science 357(6347):185–187. https://doi.org/10.1126/science.aal3999. arXiv:1707.04335 [astro-ph.SR]
Toriumi S, Iida Y, Kusano K et al (2014) Formation of a flare-productive active region: observation and numerical simulation of NOAA AR 11158. Sol Phys 289(9):3351–3369. https://doi.org/10.1007/s11207-014-0502-1. arXiv:1403.4029 [astro-ph.SR]
van Ballegooijen AA (1982) The overshoot layer at the base of the solar convective zone and the problem of magnetic flux storage. Astron Astrophys 113:99–112
Vasil GM, Brummell NH (2008) Magnetic buoyancy instabilities of a shear-generated magnetic layer. Astrophys J 686(1):709–730. https://doi.org/10.1086/591144
Vasil GM, Brummell NH (2009) Constraints on the magnetic buoyancy instabilities of a shear-generated magnetic layer. Astrophys J 690(1):783–794. https://doi.org/10.1088/0004-637X/690/1/783
Vögler A, Shelyag S, Schüssler M et al (2005) Simulations of magneto-convection in the solar photosphere. Equations, methods, and results of the MURaM code. Astron Astrophys 429:335–351. https://doi.org/10.1051/0004-6361:20041507
Wang YM, Sheeley NR Jr (1989) Average properties of bipolar magnetic regions during sunspot cycle 21. Sol Phys 124(1):81–100. https://doi.org/10.1007/BF00146521
Weber MA, Browning MK (2016) Modeling the rise of fibril magnetic fields in fully convective stars. Astrophys J 827(2):95. https://doi.org/10.3847/0004-637X/827/2/95. arXiv:1606.00380 [astro-ph.SR]
Weber MA, Fan Y, Miesch MS (2011) The rise of active region flux tubes in the turbulent solar convective envelope. Astrophys J 741(1):11. https://doi.org/10.1088/0004-637X/741/1/11. arXiv:1109.0240 [astro-ph.SR]
Weber MA, Fan Y, Miesch MS (2013a) A theory on the convective origins of active longitudes on solar-like stars. Astrophys J 770(2):149. https://doi.org/10.1088/0004-637X/770/2/149. arXiv:1305.1904 [astro-ph.SR]
Weber MA, Fan Y, Miesch MS (2013b) Comparing simulations of rising flux tubes through the solar convection zone with observations of solar active regions: constraining the dynamo field strength. Sol Phys 287(1–2):239–263. https://doi.org/10.1007/s11207-012-0093-7. arXiv:1208.1292 [astro-ph.SR]
Weber MA, Browning MK, Boardman S et al (2017) The suppression and promotion of magnetic flux emergence in fully convective stars. In: Nandy D, Valio A, Petit P (eds) Living around active stars. IAU Symposium, vol 328. Cambridge University Press, pp 85–92. https://doi.org/10.1017/S1743921317003830. arXiv:1703.04982
Wright NJ, Drake JJ (2016) Solar-type dynamo behaviour in fully convective stars without a tachocline. Nature 535(7613):526–528. https://doi.org/10.1038/nature18638. arXiv:1607.07870 [astro-ph.SR]
Yeates AR, Muñoz-Jaramillo A (2013) Kinematic active region formation in a three-dimensional solar dynamo model. Mon Not R Astron Soc 436(4):3366–3379. https://doi.org/10.1093/mnras/stt1818. arXiv:1309.6342 [astro-ph.SR]

Authors and Affiliations

Maria A. Weber[1] · Hannah Schunker[2] · Laurène Jouve[3] · Emre Işık[4,5]

✉ M.A. Weber
mweber@deltastate.edu

✉ E. Işık
isik@mps.mpg.de

H. Schunker
hannah.schunker@newcastle.edu.au

L. Jouve
ljouve@irap.omp.eu

1 Division of Mathematics and Sciences, Delta State University, 1003 W Sunflower Rd, Cleveland, 38733, MS, United States

2 School of Information and Physical Sciences, University of Newcastle, University Drive, Callaghan, 2308, NSW, Australia

3 IRAP/OMP/CNRS, Université Toulouse 3, 14 Avenue Edouard Belin, Toulouse, 31400, France

4 Max-Planck-Institut für Sonnensystemforschung, Justus-von-Liebig-Weg 3, 37077, Göttingen, Germany

5 Department of Computer Science, Turkish-German University, Şahinkaya Cd. 94, Beykoz, 34800, Istanbul, Turkey